

Magnetohydrodynamic experiments on cosmic magnetic fields

Frank Stefani^{1,*}, Agris Gailitis^{2,**}, and Gunter Gerbeth^{1***}

¹ Forschungszentrum Dresden-Rossendorf, P.O. Box 510119 Dresden, Germany

² Institute of Physics, University of Latvia, LV-2169 Salaspils 1, Latvia

Received XXXX, revised XXXX, accepted XXXX

Published online XXXX

Key words Magnetohydrodynamics, Dynamo, Magnetorotational instability

MSC (2000) 04A25

It is widely known that cosmic magnetic fields, i.e. the fields of planets, stars, and galaxies, are produced by the hydromagnetic dynamo effect in moving electrically conducting fluids. It is less well known that cosmic magnetic fields play also an active role in cosmic structure formation by enabling outward transport of angular momentum in accretion disks via the magnetorotational instability (MRI). Considerable theoretical and computational progress has been made in understanding both processes. In addition to this, the last ten years have seen tremendous efforts in studying both effects in liquid metal experiments. In 1999, magnetic field self-excitation was observed in the large scale liquid sodium facilities in Riga and Karlsruhe. Recently, self-excitation was also obtained in the French "von Kármán sodium" (VKS) experiment. An MRI-like mode was found on the background of a turbulent spherical Couette flow at the University of Maryland. Evidence for MRI as the first instability of an hydrodynamically stable flow was obtained in the "Potsdam Rossendorf Magnetic Instability Experiment" (PROMISE). In this review, the history of dynamo and MRI related experiments is delineated, and some directions of future work are discussed.

Copyright line will be provided by the publisher

1 Once upon a time...

Magnetism has been known for approximately 3000 years. There is some evidence that a hematite bar, found close to Veracruz (now Mexico), had served the Olmecs as a simple compass [29]. In any case, the Chinese have built, probably in the first century B.C., a compass in the form of a lodestone spoon that was freely turnable on a polished bronze plate [155]. The old Greek philosophers, starting with Thales of Miletus [2], were well aware of the attracting forces of lodestone, and the Roman philosopher Lucretius (95?-55 B.C.) described its action in an atomistic way [140]: "First, stream there must from off the lode-stone seeds. Innumerable, a very tide, which smites by blows that air asunder lying betwixt the stone and iron. And when is emptied out this space, and a large place between the two is made a void, forthwith the primal germs of iron, headlong slipping, fall conjoined into the vacuum, and the ring itself by reason thereof doth follow after and go thuswise with all its body."

As early as 1269, a first systematic experimental study of the attracting and repelling forces of lodestone was published by Petrus Peregrinus in his "Epistola de magnete" [169]. For the first time, he defined the concept of polarity and distinguished the north and south poles of the magnet. He was the first to formulate the law that poles of opposite polarity attract while poles of the same polarity repel each other (cf. Figure 1a). Besides the construction of several compasses (cf. Figure 1b), he also proposed a magnetic perpetuum mobile.

Three centuries later, Peregrinus' work inspired William Gilbert to make his own experiments with small spheres of lodestone ("terrellae"), which led him, in 1600, to the conclusion that "...that the terrestrial globe is magnetic and is a loadstone [79]"

However, this lodestone theory soon ran into trouble when the westward drift of the Earth's magnetic field declination was described by Gellibrand in 1635 [76], and the detection of abrupt polarity reversals by David and Brunhes in 1904/05 [21] has dealt it the ultimate deathblow.

Interestingly, it was not the well-studied magnetic field of the Earth, but the observation of magnetic fields in sunspots [87], that put Larmor on the right track speculating [127] that it could be "...possible for the internal cyclic motion to act after the manner of the cycle of a *self-exciting dynamo*, and maintain a permanent magnetic field from insignificant

* Corresponding author, e-mail: F.Stefani@fzd.de, Phone: +49 351 260 3069, Fax: +49 351 260 2007

** gailitis@sal.lv

*** G.Gerbeth@fzd.de

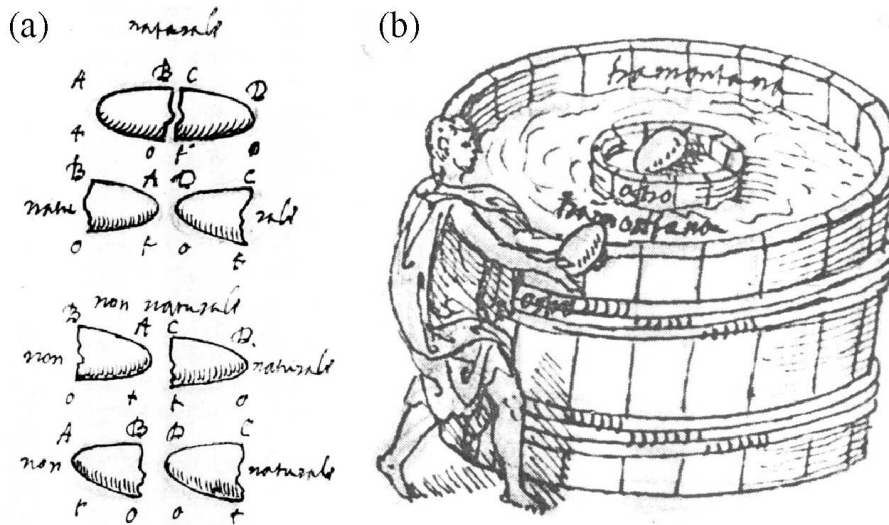


Fig. 1 Lodestone experiments of Petrus Peregrinus. (a) Experiments showing the attracting and repelling forces of a broken piece of lodestone. Upper configuration: "naturale", lower configuration: "non naturale". (b) A simple compass. Figures from [169].

beginnings, at the expense of some of the energy of the internal circulation." This one-page communication, in which a natural process was explained in terms of a technical device [208, 209, 257], was the birth certificate of the modern hydromagnetic theory of cosmic magnetic fields.

2 Cosmic magnetism

Wherever in the cosmos a large quantity of an electrically conducting fluid is found in convection, one can also expect a magnetic field to be around.

The Earth is not the only planet in the solar system with a magnetic field [144, 233]. Fields are produced inside the gas giants Jupiter, Saturn and the ice giants Uranus, and Neptune. Possibly, a dynamo had worked inside Mars in the ancient past [41]. The Mariner 10 mission in 1974-75 had revealed the magnetic field of Mercury [156] and there remain many puzzles as to how it can be produced [212, 35, 81, 82]. The detection of the magnetic field of Ganymede, the largest Jupiter moon, was one of the major discoveries of NASA's Galileo spacecraft mission in 1996 [114]. The fact that Venus does not have a dynamo generated magnetic field has been attributed to the very slow rotation [144], but also to the stably stratified liquid core [232] of this planet.

The magnetic fields of sunspots were discovered by Hale (1908) at Mt. Wilson observatory, thus proving evidence that natural magnetism is not a phenomenon restricted to the Earth. With view on the tight relation of sunspots and magnetic fields, sunspot observation turns into a perfect test field for any theory of solar magnetism. Still today, the 11 year periodicity of sunspots, their migration towards the equator (the "butterfly diagram"), and the occurrence of grand minima which are superimposed upon the main periodicity are the subject of intensive investigations [160].

Some main-sequence stars of spectral type A have remarkable magnetic field strengths on the order of 1 T which are hardly explainable by dynamo action and which have been claimed to be remnants of the star's formation, i.e. "fossil fields" [17]. However, this magnetic field strength is rather moderate compared with that of other stars. The field of some white dwarfs can easily reach values of 100 T, and even fields of 10^{11} T have been ascribed to some anomalous X-ray emitting pulsars [117].

Large-scale magnetic fields of the order of 10^{-9} T are observed in many spiral galaxies [11]. Usually there is a close correlation of the magnetic field structure with the spiral pattern that indicates the relevance of dynamo action, although by far not all problems with the origin and amplitude of galactic seed fields are solved [85, 123, 48].

Fascinating phenomena appear close to the centers of galaxies which are usually occupied by supermassive black holes. These are fed by so-called accretion disks [9], a process which results typically in two oppositely directed jets of high-energetic particles that can fill vast volumes with magnetic field energy [120]. In our galaxy, these jets are rather weak but show a particularly interesting feature. Morris et al. recently reported the detection of a double-helix nebula in this outflow,

not far from the galactic center, which they described as an Alfvén wave [148]. However, we will see later that this might well be connected with a typical dynamo action.

The working principle of accretion disks, which are the most efficient "powerhouses" in the universe [88] supplying energy for systems such as X-ray binaries, active galactic nuclei, and quasars through the release of gravitational potential energy, had been a puzzle for a long time. The problem is that matter, before it can be accreted by the central object, has to get rid off its angular momentum. The molecular viscosity of such gas disks is much too small to explain the observed accretion rates of stars and black holes, so that turbulent viscosity has to be assumed [204]. The point is only: why accretion disks are turbulent at all? Since they obey Kepler's third law, i.e., their angular velocity decays as $r^{-3/2}$ with the radius, while the angular momentum increases as $r^{1/2}$, Rayleigh's criterion must be applied stating that rotating flows with radially increasing angular momentum are linearly stable for all Reynolds numbers [184]. In principle, the solution to this puzzle was already given in papers by Velikhov in 1959 [247] and Chandrasekhar in 1960 [30], who had detected that a Taylor-Couette flow in the hydrodynamically stable regime could be destabilized by an axially applied magnetic field. The astrophysical importance of this "magnetorotational instability" was, however, noticed by Balbus and Hawley in their seminal paper of 1991 [7].

Going beyond the galactic scale, we find randomly tangled magnetic fields also in galaxy clusters [84] which brings us to the topic of *fluctuation dynamos* (or *small-scale dynamos*) which have attracted much interest recently [198, 199].

3 Some mathematical basics

The temporal evolution of the velocity field \mathbf{v} under the influence of a magnetic field \mathbf{B} is governed by the Navier-Stokes equation

$$\frac{\partial \mathbf{v}}{\partial t} + (\mathbf{v} \cdot \nabla) \mathbf{v} = -\frac{\nabla p}{\rho} + \frac{1}{\mu_0 \rho} (\nabla \times \mathbf{B}) \times \mathbf{B} + \nu \Delta \mathbf{v} + \mathbf{f}_d, \quad (1)$$

where ρ and ν denote the density and the kinematic viscosity of the fluid, p is the pressure, μ_0 the magnetic permeability of the vacuum, and \mathbf{f}_d symbolizes driving forces as, e.g., buoyancy in cosmic bodies or mechanical forcing by propellers in liquid metal experiments. The magnetic field \mathbf{B} in equation (1) is in general the sum of an externally applied magnetic field and the flow induced or self-excited magnetic field.

In order to derive the temporal evolution for \mathbf{B} in a fluid of electrical conductivity σ , we start with Ampère's law, Faraday's law, the divergence-free condition for the magnetic field, and Ohm's law in moving conductors:

$$\nabla \times \mathbf{B} = \mu_0 \mathbf{j} \quad (2)$$

$$\nabla \times \mathbf{E} = -\dot{\mathbf{B}} \quad (3)$$

$$\nabla \cdot \mathbf{B} = 0 \quad (4)$$

$$\mathbf{j} = \sigma(\mathbf{E} + \mathbf{v} \times \mathbf{B}). \quad (5)$$

Here, \mathbf{E} denotes the electric field and \mathbf{j} denotes the electric current density. We have skipped the displacement current in equation (2) as in most relevant cases the quasistationary approximation holds. Taking the *curl* of equations (2) and (5), inserting equation (3), and assuming σ to be constant in the considered region, one readily arrives at the *induction equation* for the magnetic field:

$$\frac{\partial \mathbf{B}}{\partial t} = \nabla \times (\mathbf{v} \times \mathbf{B}) + \frac{1}{\mu_0 \sigma} \Delta \mathbf{B}. \quad (6)$$

Obviously, the right hand side of equation (6) describes the competition between the diffusion and the advection of the field. For $\mathbf{v} = 0$ equation (6) reduces to a vector heat equation and the field will decay within a typical time $t_d = \mu_0 \sigma l^2$, with l being a typical length scale of the considered system. Switching on the advection term, it can lead to an increase of \mathbf{B} within a kinematic time $t_k = l/v$, where v is a typical velocity of the flow. If the kinematic time is smaller than the diffusion time, the net effect can become positive, and the field will grow. Comparing the diffusion time-scale with the kinematic time-scale we get a dimensionless number that governs the "fate" of the magnetic field which is called magnetic Reynolds number Rm :

$$Rm := \mu_0 \sigma l v. \quad (7)$$

Depending on the flow pattern, the values of the critical Rm , at which the field starts to grow, are usually in the range of $10^1 \dots 10^3$. Most flows in cosmic bodies, in which Rm is large enough, will act as dynamos, although there are a number of anti-dynamo theorems excluding too simple structures of the velocity field or the self-excited magnetic field [42, 51, 189, 97, 104].

The competition between field dissipation and production can also be understood in terms of the energy balance. Taking the scalar product of the induction equation with \mathbf{B}/μ_0 , and performing an integration by parts, we find for the time evolution of the magnetic energy

$$\frac{d}{dt} \int_V \frac{\mathbf{B}^2}{2\mu_0} dV = - \int_V \mathbf{v} \cdot (\mathbf{j} \times \mathbf{B}) dV - \int_V \frac{\mathbf{j}^2}{\sigma} dV - \frac{1}{\mu_0} \oint_S (\mathbf{E} \times \mathbf{B}) \cdot d\mathbf{S}. \quad (8)$$

In this form, the dynamo action can be interpreted in a convenient way: the time derivative of the magnetic field energy equals the difference between the work done (per time) by the Lorentz forces on one side and the Ohmic and Poynting flux losses on the other side. The Lorentz force converts kinetic energy into magnetic energy, the Ohmic dissipation converts magnetic energy into heat, the Poynting flux transports electromagnetic energy across the surface S of the considered volume V .

Besides the magnetic Reynolds number Rm , the coupled system of Eqs. (1) and (6) is governed by some more dimensionless numbers: first of all the well known Reynolds number $Re := lv/\nu$, second the Hartmann number $Ha := Bl\sqrt{\sigma/\nu\rho}$ which describes the square root of the ratio of magnetic to viscous forces. In some cases, the system behaviour is better described by the interaction parameter (Stuart number) $N = \sigma B^2 l / (\nu\rho) = Ha^2 / Re$ or the Lundquist number $S =: Bl\sigma\sqrt{\mu_0/\rho} = Ha\sqrt{Pm}$, wherein the magnetic Prandtl number is defined as the ratio of kinematic viscosity to magnetic diffusivity: $Pm := \nu\mu_0\sigma$. Of course, more dimensionless numbers will enter the scene when a particular forcing and/or global rotation of the system is taken into account.

The coupled system of equations (1) and (6) can be treated with varying complexity. For many technologically relevant cases, but also for the "helical MRI" to be discussed later, with $Rm \ll 1$, it will suffice to use the so-called inductionless approximation [173]. On the other extreme, one can study "kinematic dynamo models" by just solving equation (6) while supposing \mathbf{v} to be fixed. In general, however, the treatment of most magnetic instabilities and of dynamically consistent dynamos requires the simultaneous solution of equations (1) and (6).

The numerical costs of the simulations are strongly governed by the relevant spatial dimension of the considered system. In some cases, including long cylindrical dynamos with axially invariant flows or long MRI experiments based on Taylor-Couette flows, it is appropriate to start with an analysis of normal modes in axial and azimuthal directions giving an eigenvalue problem in r direction only. For dynamo or MRI experiments in finite cylinders, 2D models in r, z will be appropriate. Most expensive are, of course, fully coupled 3D simulations of Eqs. (1) and (6).

Dynamo relevant flows are in general turbulent, the question is only about the turbulence level and its role in the dynamo process. Commonly, one distinguishes between so-called *laminar* and *mean-field* dynamo models. Laminar models are described by the unchanged equation (6) with neglected turbulence. The self-excited magnetic field varies on the same length scale as the velocity field does. Mean-field dynamo models, on the other hand, are relevant for highly turbulent flows. In this case the velocity and the magnetic field are considered as superpositions of mean and fluctuating parts, $\mathbf{v} = \bar{\mathbf{v}} + \mathbf{v}'$ and $\mathbf{B} = \bar{\mathbf{B}} + \mathbf{B}'$. From equation (6) we get the equation for the mean part $\bar{\mathbf{B}}$,

$$\frac{\partial \bar{\mathbf{B}}}{\partial t} = \nabla \times (\bar{\mathbf{v}} \times \bar{\mathbf{B}} + \mathcal{E}) + \frac{1}{\mu_0\sigma} \Delta \bar{\mathbf{B}}. \quad (9)$$

This equation for the mean field is identical to equation (6) for the original field, except for one additional term

$$\mathcal{E} = \overline{\mathbf{v}' \times \mathbf{B}'}, \quad (10)$$

that represents the mean electromagnetic force (emf) due to the fluctuations of the velocity and the magnetic field. The elaboration of mean-field dynamo models in the sixties by Steenbeck, Krause and Rädler [216] was a breakthrough in dynamo theory (cf. [119, 180]). They had shown that, for homogeneous isotropic turbulence, the mean electromotive force takes on the form

$$\mathcal{E} = \alpha \bar{\mathbf{B}} - \beta \nabla \times \bar{\mathbf{B}}, \quad (11)$$

with a parameter α that is non-zero only for non-mirrorsymmetric velocity fluctuations \mathbf{v}' ("cyclonic motion" [161]) and a parameter β that describes the enhancement of the electrical resistivity due to turbulence. The fact that helical fluid motion can induce an emf that is *parallel* to the magnetic field is now commonly known as the α -effect. Dynamo models based on the α -effect have played an enormous role in the study of solar and galactic magnetic fields, and we will later explain the physics of the Karlsruhe experiment in terms of a mean-field model with the α -effect.

A promising way to combine the credibility of direct numerical simulations with the convenience (and robustness) of mean-field models is to carry out global 3D simulations at affordable spatial resolution, and to extract then the mean-field coefficients by means of a test-field method [202, 203, 77, 19].

4 Why doing liquid metal experiments?

During recent decades tremendous progress has been made in the analytical understanding and the numerical treatment of flows with high Rm , including dynamos, which has been reported in dozens of monographs and review articles [24, 145, 119, 95, 190, 191, 31, 91, 144, 50, 192, 25, 26, 193, 18].

As for the geodynamo, to take one example, recent numerical simulations [83, 103, 122, 27, 33, 36, 254, 230, 89, 4, 231] share their main results with features of the Earth's magnetic field, including the dominance of the axial dipolar component, weak non-dipolar structures, and, in some cases, full polarity reversals, a behaviour that is well known from paleomagnetic measurements (for a recent overview, see [116]).

Despite those successes, a number of unsolved problems remain. The simulations of the Earth's dynamo, to remain in this picture for the moment, are carried out in parameter regions far from the real one. This concerns, in particular, the Ekman number E (the ratio of the rotation time scale to the viscous time scale) and the magnetic Prandtl number Pm (the ratio of the magnetic diffusion time to the viscous diffusion time). The Ekman number of the Earth is of the order 10^{-15} , the magnetic Prandtl number is of the order 10^{-6} . Present numerical simulations are carried out for values as small as $E \sim 10^{-5}$ and $Pm \sim 0.1$. The wide gap between real and numerically tractable parameters is, of course, a continuing source of uncertainty about the physical reliability of those simulations. The usual way in fluid dynamics to deal with parameter discrepancies of this sort, namely to apply sophisticated turbulence models, is presently hampered by the lack of validated turbulence models for fluids that are both fast rotating and strongly interacting with a magnetic field. Here is the crucial point where laboratory experiments are unavoidable in order to collect knowledge about the turbulence structure in the (rotating or not) dynamo regime.

With this critical attitude towards simulations, one must likewise admit that none of the real cosmic bodies can be put into a *Bonsai form* to be studied in laboratory. Taking again the geodynamo as a (striking) example, it is not possible to actualize all of the dimensionless numbers in an equivalent experimental set-up. A liquid sodium experiment of 1 m radius would have to rotate with 10^8 (!) rotations per second in order to reach the Ekman number of the Earth, which amounts to twice the speed of light at the rim of the vessel.

So what, then, can we actually learn from liquid metal experiments ?

First, it is worthwhile to verify experimentally that hydromagnetic dynamos work at all. In theory and numerics, kinematic dynamo action has been proved for a large variety of more or less smooth velocity fields or pre-described distributions of turbulence parameters. However, liquid metal flows, at the necessary Rm , will be highly turbulent. Further, most dynamo simulations have been carried out in spherical geometry. What happens when we are using cylindrical vessels instead of spheres? How important is the correct implementation of the non-local boundary conditions for the magnetic field, which is trivial for spherical geometry but requires sophisticated methods in other, e.g. cylindrical, geometry [220, 259, 260, 96, 86, 80, 78]? Later, when discussing the VKS dynamo, we will see that even slight modifications of the experimental design can teach a lot about the role of turbulence, boundary conditions, and the distribution of different dynamo sources.

Second, if one was lucky to make a hydromagnetic dynamo running, how can the exponential field growth be stopped, how does the dynamo saturate? Roughly speaking, dynamo saturation is nothing than an application of Lenz's rule stating that an induced current acts against the source of its own generation. How this saturation works in detail, depends strongly on the mechanical constraints the flow is experiencing. All of the present laboratory dynamos comprise mechanical installations to drive and guide the flow (propellers, guiding blades, etc.). Obviously, the fewer installations are present in the fluid, the more freedom has the flow to be modified and re-organized by the Lorentz forces. It would be most interesting to drive the flow purely by convection, as in the Earth's outer core. However, it seems to be impossible to reach velocities sufficient for dynamo action in a purely convective way in laboratory experiments, as discussed, e.g. in [240]. Hence, all present laboratory experiments have to find a compromise between a mechanical forcing of the flow and the degree of freedom of the flow for the magnetic field back-reaction.

This brings us to the *third* point: Besides its influence on the large scale flow, the magnetic field back-reaction may also change the turbulence properties of the flow. Sometimes this effect is considered the most important one that dynamo experiments may help to understand, as they provide an interesting test-case for MHD turbulence models (a summary of the latter can be found in [249]). Those models, once validated, could gain reliability when applied to such hard problems as magnetic field generation in the Earth's core. But "turbulence model validation" sounds much easier as it is in reality. Even the simple flow measurement in liquid sodium is a problem in its own right, let alone the measurements of all sorts of correlation functions which might be important for the validation of turbulence models.

A *fourth* topic, which is intimately connected with the issue of turbulence modification, is the destabilizing role magnetic fields can have on flows. Typically dynamo experiments and experiments on the magnetorotational instability are of a similar size, making it worth to hunt for new instabilities in the presence of (self-excited or externally applied) magnetic fields. In addition to this, there is a large variety of wave phenomena to be studied in rotating magnetized flows.

A *fifth* issue that could possibly be addressed by dynamo experiments has to do with the distinction between steady and oscillatory dynamo states. Typically, these transitions occur at so-called exceptional points of the spectrum of the non-selfadjoint dynamo operator, and polarity reversals have been described as noise triggered relaxation oscillations in the vicinity of such points [221, 222, 224]. However, reversals can occur for a wide variety of bistable systems [94], and experiments can be helpful to distinguish between different reversal scenarios.

5 The experiments in detail

In the following we will concentrate on the most important experimental efforts related to the understanding of the origin and the action of cosmic magnetic fields. We will start with the four experiments that have already shown homogeneous dynamo action, and then move to experiments devoted to wave phenomena and magnetic instabilities in liquid metals. For the sake of shortness, we have to skip some very interesting older experiments like those of Lehnert [130] (cf. [131] for a very amazing account of these experiments in Stockholm) and Gans [74], but also the impressive series of liquid metal experiments on Alfvén waves which have been summarized by Gekelmann [75]. Another topic omitted is the search for self-excitation phenomena in fast breeder reactors [13, 171, 111, 1, 170], although this close connection was occasionally used as a political argument to motivate dynamo experiments (see [218]). Slightly focusing on some newer experimental activities, we advise the reader to consult some former reviews on earlier experiments [190, 25, 128, 69, 70, 39, 240, 49, 168, 72].

For decades, hydromagnetic dynamo experiments seemed to be at the edge of technical feasibility. The problem to achieve self-excitation is that values of the critical Rm for different flow geometries are of the order of 100. For the best liquid metal conductor, sodium, the product of conductivity and magnetic permeability is approximately 10 s/m^2 . Hence, to get an Rm of 100, the product of length and velocity has to be $10 \text{ m}^2/\text{s}$. To reach this value one should have more than 1 m^3 sodium and use at least 100 kW of mechanical power to move it. Another possibility is of course to increase Rm by simply using materials with a high magnetic permeability. This brings us directly to the first experiment on homogeneous, though not hydromagnetic, dynamo action.

5.1 The dynamo experiments of Lowes and Wilkinson

In the sixties of the 20 century, Lowes and Wilkinson have carried out a long-term series of homogeneous dynamo experiments [138, 139, 255] at the University of Newcastle upon Tyne. The main idea of their experiments was already laid down in a 1958 paper by Herzenberg [90] who had given the first rigorous existence prove for a homogeneous dynamo consisting of two rotating small spheres embedded in a large sphere (Figure 2a). Thus motivated, Lowes and Wilkinson started with the first homogeneous dynamo using two rotating cylinders in a “house-shaped” surrounding conductor (Figure 2b). The key point for the success of this and the following experiments was the utilization of various ferromagnetic materials (perminvar, mild steel, electrical iron) making the magnetic Reynolds number large, simply by a high relative magnetic permeability μ_r (between 150 and 250).

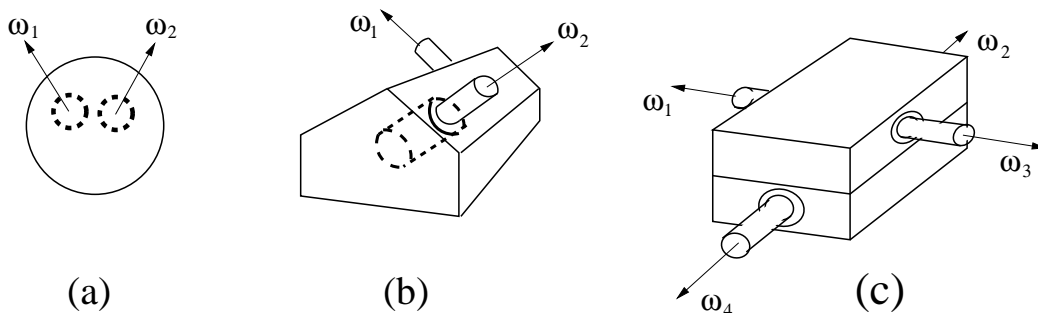


Fig. 2 (a) The Herzenberg dynamo. Two spheres rotate around non-parallel axes. (b) The first dynamo of Lowes and Wilkinson. Two cylinders rotate in a “house-shaped” block. (c) The fifth dynamo with four independent rotors.

The history of these experiments is impressive, not only for their step-by-step improvements but also for the continuing comparison of the resulting field with geomagnetic features [255]. Starting with a simple geometry of the rotating cylinders (Figure 2b), which produced steady and oscillating magnetic fields, the design was made more sophisticated (Figure 2c) so that finally it permitted the observation of field reversals. That way it was shown that a complex field structure and behaviour can result from comparatively simple patterns of motion.

Needless to say, the experiments were flawed by the use of ferromagnetic materials and the nonlinear field behaviour which is inevitably connected with these materials. One attempt to get self-excitation with rotating non-magnetic copper

cylinders failed. And, although homogeneous, these dynamos were not suited to study the nontrivial back-reaction of the magnetic field on the fluid motion, and there was no chance to learn something about MHD turbulence.

5.2 The dynamo experiments in Riga

There is a long tradition at the Institute of Physics Riga, Latvia, to carry out dynamo related experiments.

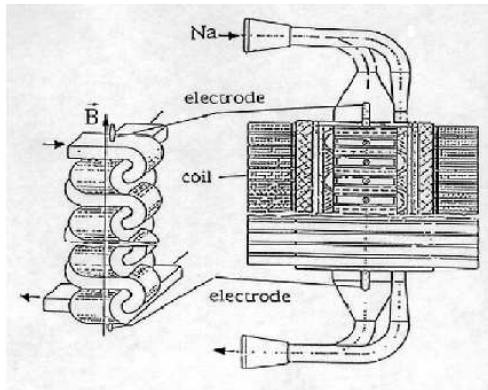


Fig. 3 The “ α -box,” the first dynamo-related experiment in Riga. The sodium flow through the helically interlaced channels produces an emf parallel to the applied magnetic field.

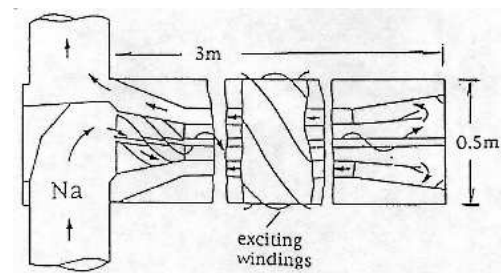


Fig. 4 The dynamo module of the 1987 experiment. Significant amplifications of externally applied magnetic fields were measured, before the experiment had to be stopped due to mechanical vibrations.

The first one, actually proposed by Max Steenbeck, was intended to prove experimentally the α effect, i.e. the induction of an electromotive force parallel to an applied magnetic field. This experiment, the “ α -box” (Figure 3), consisted of two orthogonally interlaced copper channels through which sodium was pumped with velocities up to 11 m/s. Interestingly, although the very flow helicity $\mathbf{v} \cdot (\nabla \times \mathbf{v})$ is zero everywhere in this set-up, an α effect results from the non-mirror-symmetry of the flow. The main result of this experiment was that the induced voltage between the electrodes (cf. Figure 3) is proportional to v^2 , i.e., it is independent of the flow direction, and that it reverses if the applied magnetic field is reversed. The α -effect was therefore validated [217]. Interestingly, the induced current was shown to increase slower than linearly with the applied magnetic field, a result which points to some quenching of α with increasing interaction parameter.

A second experiment was also prepared in Riga but actually carried out in St. Petersburg in 1986 [62] (Figure 4). The principle idea of this, as well as of the later Riga dynamo experiment, traces back to Ponomarenko [172] who had proved that a helically moving, electrically conducting cylinder embedded in an infinite stationary conductor can show dynamo action. This simple configuration was analyzed in more detail by Gailitis and Freibergs [60] who found a remarkably low critical magnetic Reynolds number of 17.7 for the convective instability. By adding a back-flow, this convective instability can be transformed into an absolute instability [61].

All this early numerical work, including the optimization [59] of the main geometric relations which led to the design of the Riga dynamo (Figure 5a,b), was done with a one-dimensional eigenvalue solver. For refined kinematic simulations a two-dimensional finite difference code (in radial and axial direction) was written whose main advantage is the possibility to treat velocity structures varying in axial direction, which is indeed of relevance for the Riga dynamo [71]. The magnetic field structure as it comes out of this code is illustrated in Figure 5c.

Much effort has been spent to fine-tune the whole facility. The first step was to optimize the main geometric relations, in particular the relations of the three radii to each other and to the length of the system [59]. The resulting shape of the central module of the dynamo is shown in Figure 5b. In a water dummy facility at the Dresden Technical University, many tests have been carried out to optimize the velocity profiles [32] and to ensure the mechanical integrity of the system. All the experimental preparations were accompanied by extensive numerical simulations. One main result of these simulations was the optimization of the velocity profile with regard to the limited motor power resources of around 200 kW. For helicity maximizing profiles (“Bessel function profiles”) a critical Rm as low as 12.0 (for the convective instability) and 14.7 (for the absolute instability) has been found, while the corresponding numbers for the measured (as far as possible optimized) profiles were 14.3 and 17.6, respectively [219]. Another result was the prediction of the main features of the expected magnetic field, i.e., its growth rate, frequency, and spatial structure, and the dependence of these features on the rotation rate of the propeller.

At the present facility, eight experimental campaigns have been carried out between November 1999 and July 2007. In the first campaign in November 1999, a self-exciting field was documented for the first time in a liquid metal dynamo experiment, although the saturated regime could not be reached at that time [64]. This had to be left until the July 2000

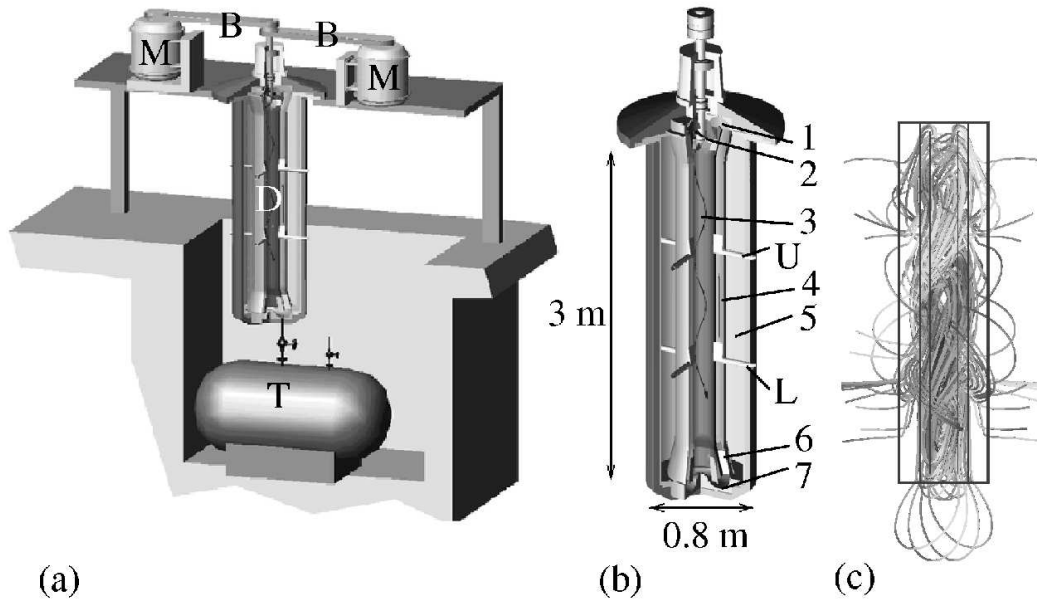


Fig. 5 The Riga dynamo experiment and its eigenfield. (a) Sketch of the facility. M - Motors. B - Belts. D - Central dynamo module. T - Sodium tank. (b) Sketch of the central module. 1 - Guiding blades. 2 - Propeller. 3 - Helical flow region without any flow-guides, flow rotation is maintained by inertia only. 4 - Back-flow region. 5 - Sodium at rest. 6 - Guiding blades. 7 - Flow bending region. (c) Simulated magnetic eigenfield. The gray scale indicates the vertical component of the field.

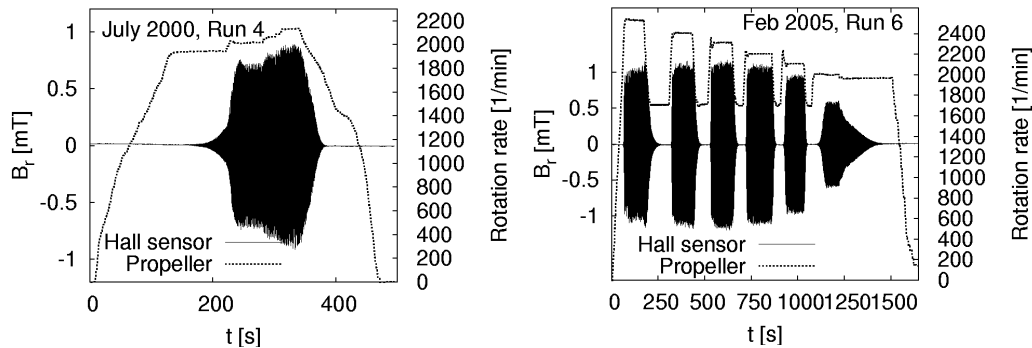


Fig. 6 Two experimental runs carried out in July 2000 and in February 2005. Rotation rate of the motors, and magnetic field measured at one Hall external sensor plotted vs. time. After the exponential increase of the magnetic field in the kinematic dynamo regime, the dependence of the field level on the rotation rate has been studied in the saturation regime.

experiment [65]. In June 2002, the radial dependence of the magnetic field was determined by the use of Hall sensors and induction coils situated on "lances" going throughout the whole dynamo module. In February and June 2003, first attempts were made to measure the Lorentz force induced motion in the outermost cylinder. A novelty of the May 2004 campaign was the measurements of pressure in the inner channel by a piezoelectric sensor that was flash mounted at the innermost wall. In February/March 2005, a newly developed permanent magnet probe was inserted into the innermost cylinder in order to get information about the velocity there, and two traversing rails with induction coils and Hall sensors were installed to get continues field information along the z -axis and across the whole diameter of the dynamo. In July 2007, a newly developed magnetic coupler was installed to replace the outworn gliding ring seal. More details about these results can be found in Refs. [69, 71, 68, 66, 67, 70], and will also be published elsewhere.

In Figure 6 we document two experimental runs carried out in July 2000 and in February 2005. It is clearly visible that the magnetic field switches on and off when a critical value of the propeller rotation rate is crossed from below or above, respectively.

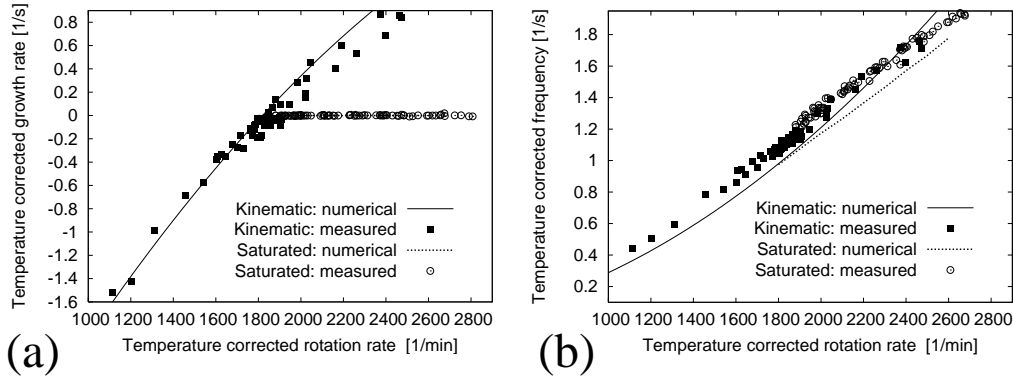


Fig. 7 Measured growth rates and frequencies of the magnetic eigenfield for different rotation rates Ω in the kinematic and the saturation regime, compared with the numerical predictions. Ω , p , and f at the temperature T were scaled to $(\Omega_s, p_s, f_s) = \sigma(T)/\sigma(157^\circ\text{C}) (\Omega(T), p(T), f(T))$ as required by the scaling properties of equation (6).

In Figure 7 the temperature corrected measurement data for the growth rate (Fig 7a) and the frequency (Fig. 7b) are shown in comparison with the corresponding numerical results. The numerical curves in the kinematic regime were obtained with the 2D solver [219, 71] and were slightly corrected by the effect of the lower conductivity of the stainless steel walls that was estimated separately by a 1D solver.

As for the saturation regime we have modelled the most important back-reaction effect within a simple one-dimensional model [68, 71]. This relies on the fact that, while the axial velocity component has to be rather constant from top to bottom due to mass conservation, the azimuthal component v_ϕ can be easily braked by the Lorentz forces without any significant pressure increase. In the inviscid approximation, and considering only the $m = 0$ mode of the Lorentz force, we end up with the ordinary differential equation for the Lorentz force induced perturbation $\delta v_\phi(r, z)$ of the azimuthal velocity component:

$$\bar{v}_z(r, z) \frac{\partial}{\partial z} \delta v_\phi(r, z) = \frac{1}{\mu_0 \rho} [(\nabla \times \mathbf{B}) \times \mathbf{B}]_\phi(r, z) . \quad (12)$$

This equation is now solved simultaneously with the induction equation, both in the innermost channel where it describes the downward braking of v_ϕ , and in the back-flow channel where it describes the upward acceleration of v_ϕ . Both effects together lead to a reduction of the differential rotation and hence to a deterioration of the dynamo capability of the flow. The validity of this self-consistent back-reaction model, which gives automatically a zero growth rate, can be judged from the dependence of the resulting eigenfrequency in Figure 7b. Actually, we see a quite reasonable correspondence with the measured data, in particular with respect to the slope of the curve.

Only recently, a sophisticated T-RANS (transient Reynolds average Navier-Stokes equation) model of the Riga dynamo experiment has been developed at the Delft Technical University [105, 106, 107]. This model, which incorporates the state of the art of hydrodynamic turbulence modelling under the influence of magnetic fields, has basically confirmed, and slightly improved, the main predictions of our simple one-dimensional back-reaction model.

5.3 The Karlsruhe dynamo experiment

Historically it is interesting that not only the basic idea and the geophysical motivation, but also a final formula for the critical flow-rates for a sort of Karlsruhe experiment can already be found in a paper of 1967 [58]. The idea was to substitute real helical ("gyrotropic") turbulence by "pseudo-turbulence" actualized by a large (but finite) number of parallel channels with a helical flow inside. Later, in 1975, Busse considered a similar kind of dynamo [23] which prompted him to initiate the Karlsruhe dynamo experiment which was then designed and carried out by R. Stieglitz and U. Müller.

In 1972, Roberts had proved dynamo action for a velocity pattern periodic in x and y that comprises both a rotational flow and an axial flow [188]. The α -part of the electromotive force for this flow type can be written in the form $\mathcal{E} = -\alpha_\perp (\bar{\mathbf{B}} - (\mathbf{e}_z \cdot \bar{\mathbf{B}}) \mathbf{e}_z)$, which represents an extremely anisotropic α -effect that produces only electromotive forces in the x - and y -directions, but not in the z -direction [175].

In the specific realization of the Karlsruhe experiment (Figure 8), the Roberts flow in each cell is replaced by a flow through two concentric channels. In the central channel the flow is straight, in the outer channel it is forced by a "spiral staircase" on a helical path (Figure 9). This design principle of the Karlsruhe dynamo being given, a fine tuning of the

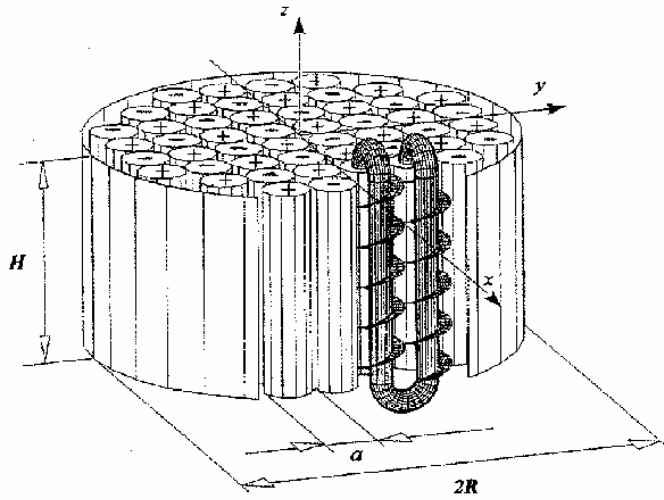


Fig. 8 Central part of the Karlsruhe dynamo facility. The module consists of 52 spin-generators, each containing a central tube with non-rotating flow and an outer tube where the flow is forced on a helical path. Figure courtesy of R. Stieglitz.

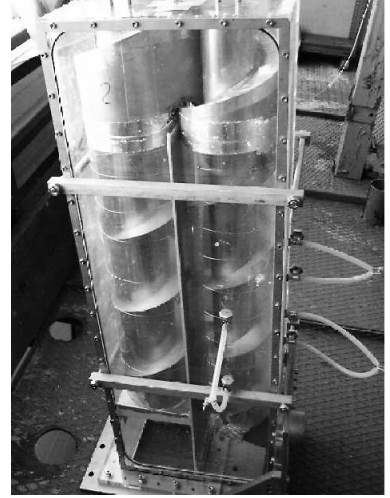


Fig. 9 A model of a spin-generator. Figure courtesy of R. Stieglitz and Th. Gundrum.

geometric relations were carried out with the aim to achieve a maximum α effect for a given power of the pumps. Such an optimization led to a number of 52 spin generators, a radius of 0.85 m and a height of 0.7 m for the dynamo module.

Figure 10 documents the experiment carried out in December 1999 [149, 234]. The scheme in Figure 10a depicts again the central dynamo module with the 52 spin-generators, and defines the coordinate system for the location and direction of the Hall probes. Figure 10b shows the measured x -component of the magnetic field. This signal was recorded after the central flow rate \dot{V}_C was set to a constant value of $115 \text{ m}^3/\text{h}$ and the flow rate \dot{V}_H in the helical ducts was increased from $95 \text{ m}^3/\text{h}$ to $107 \text{ m}^3/\text{h}$ at a time 30 s from the start of the experiment. After approximately 120 s the field starts to saturate at an approximately 7 mT.

For the experimentally interesting region, the isolines of the quantity $C = \mu_0 \sigma \alpha_{\perp} R$, which is a dimensionless measure of the α -effect, and the experimentally obtained curves, are plotted in Figure 11. The experimentally determined neutral line, separating dynamo and non-dynamo regions, corresponds to values of C^{crit} in the region of 8.4...9.3. Hence, the numerical prediction, $C^{crit} = 8.12$, resulting from mean-field theory [176], was quite reasonable.

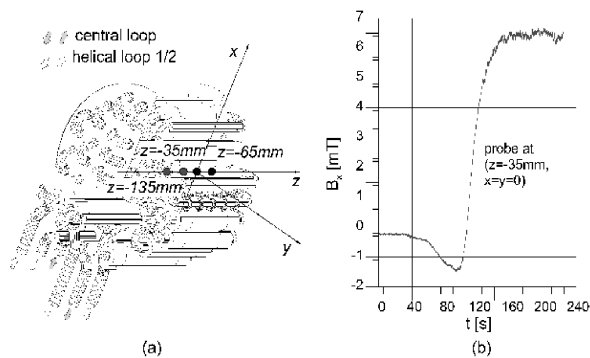


Fig. 10 Self-excitation and saturation in the Karlsruhe dynamo experiment. (a) The dynamo module with the connections between the spin-generators and the supply pipes. (b) Hall sensor signals of B_x in the inner bore of the module. Figure courtesy of R. Stieglitz.

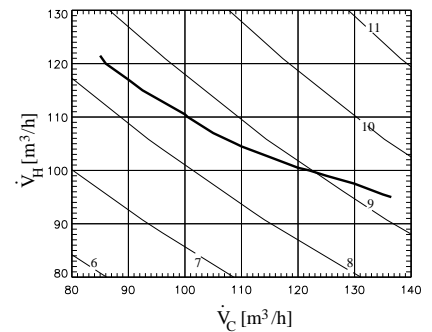


Fig. 11 Isolines of the dimensionless number $C = \mu_0 \sigma \alpha_{\perp} R$ in the $\dot{V}_C - \dot{V}_H$ -plane. In a certain approximation, dynamo action should occur beyond the isoline with $C_{crit} = 8.12$ [176]. The experimentally determined neutral line (bold), separating regions with and without dynamo action, slightly deviates from the theoretical line. Figure courtesy of K.-H. Rädler.

During its comparably short lifetime, the Karlsruhe dynamo experiment has brought about many results on its imperfect bifurcation behaviour and on MHD turbulence which are documented in [150, 151, 152]. Much work has also been done in order to predict the kinematic dynamo behaviour [238, 239, 176, 243] and to understand quantitatively the saturated regime

[241, 177, 178]. It should be mentioned that data from the Karlsruhe experiment have been used in an attempt to distinguish between two different scaling laws of the geodynamo, with interesting consequences for its power consumption [34].

A last remark: There is growing evidence that the disassembling of the Karlsruhe dynamo facility was too rash. Recent numerical simulations have shown [5] that just a very slight decrease of the aspect ratio of the dynamo module would have changed the dominant dipole direction from equatorial to axial. It suggests itself that in the vicinity of this point one could have expected quite interesting flip-flop phenomena between equatorial and axial dipoles in the non-linear regime of the dynamo. A similar point concerns transitions between steady and oscillatory dynamo regimes which typically occur at so-called exceptional points of the spectrum of the non-selfadjoint dynamo operator. Those transitions have been made responsible for the polarity reversals of the Earth's magnetic field [221, 222, 224]. In technical terms, an appropriate sign change of α along the radius of the module would have been sufficient for such a transition to occur. In any case, with modifying slightly the central module of the Karlsruhe dynamo, keeping all other parts of the installation unchanged, there would have been a good chance to investigate very interesting effects. Unfortunately, this opportunity has been missed.

5.4 The VKS experiment in Cadarache

At the CEA research center in Cadarache (France), a group lead by J.-F. Pinton (ENS Lyon), S. Fauve (ENS Paris) and F. Daviaud (CEA Saclay) has built a dynamo experiment under the acronym VKS ("von Kármán sodium"). Here, "von Kármán" stands for the flow between two rotating disks [262].

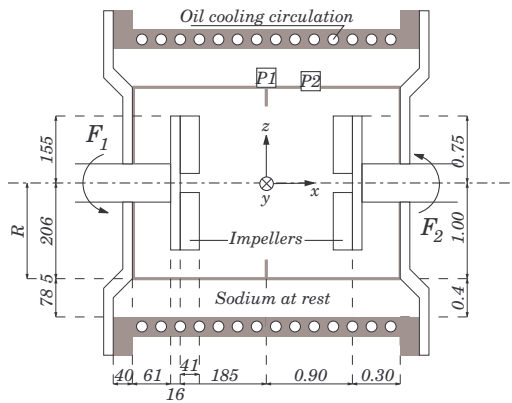


Fig. 12 Design of the VKS experiment with two disks counter-rotating in the cylinder driving two poloidal and two toroidal eddies ($s2^+t2$). The numbers on the l.h.s are the dimension in mm, the numbers on the r.h.s are the dimensions normalized by the radius. Figure courtesy of the VKS team.

In a first version of the experiment (VKS 1), the flow was produced inside a cylindrical vessel with equal diameter and height, $2R = H = 0.4$ m, driven by two 75 kW motors at rotation rates up to 1500 rpm. The von Kármán flow geometry has been chosen as it represents a convenient realization of the so-called $s2^+t2$ flow that consists of two poloidal eddies ($s2$) which are inward directed in the equatorial plane ($+$), and two counter-rotating toroidal eddies ($t2$). Such a flow is known to yield self-excitation at comparably low values of Rm [47, 154]. One problem of such flows is that the counter-rotation in the equatorial plane is a powerful source of turbulence. Although significant induction effects were measured in this first experiment [141, 15, 166, 167], no self-excitation was observed.

Based on this experience, a new version of the experiment (VKS 2) had been constructed (Figure 12). The total sodium volume was extended from 50 l to 150 l, the available motor power from 75 kW to 300 kW, and great effort was spent in order to optimize the shape of the blades of the impellers [142, 181, 143]. Further, a side layer with sodium at rest was attached which reduces the critical Rm drastically. In spite of this thorough optimization, this experiment failed to show self-excitation [183], and the induced magnetic fields turned out to be significantly weaker than numerically predicted [182]. The reason for this general under-performance was controversially discussed. One "school" attributed it to (large scale) fluctuations [129], another one attributed it to the existence of "lid layers" behind the impellers, and in particular to the sodium rotation therein [223, 261, 124].

In an attempt to mitigate this detrimental effect of lid layers, it was decided to change the axial magnetic boundary conditions by replacing the stainless steel impellers by those made of soft-iron. This modification led ultimately to the observation of self-excitation in fall 2006 [146]. In some parameter regions, characterized by asymmetric forcing with different rotation rates of the two impellers, impressive magnetic field reversals (cf. Figure 13) were recorded [12].

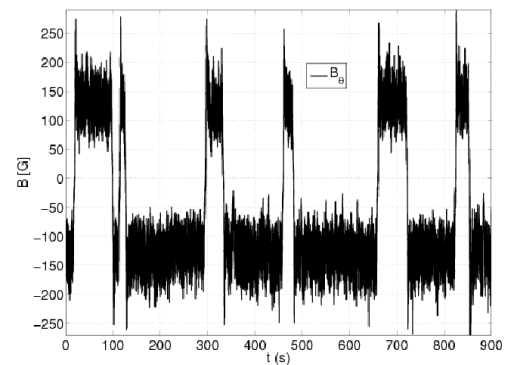


Fig. 13 A reversal of the azimuthal magnetic field occurring when the rotation rate of one propeller was 16 Hz and that of the other propeller was 22 Hz. Figure courtesy of the VKS team.

The critical Rm of the VKS 2 experiment with soft iron propellers was determined to be $\approx 31\dots35$, in contrast to the numerical predictions between 48 and 133 (the latter depending mainly on the flow details in the lid layers). The really surprising thing was, however, that the self-excited eigenfield turned out to be basically an axisymmetric one, in contradiction to the non-axisymmetric equatorial dipole that was predicted by numerics. This axisymmetric field is apparently at odds with Cowling's theorem [42] which forbids non-decaying axisymmetric eigenfields to be excited by large-scale flows.

Hence, numerical work is going on to understand better the functioning of the VKS dynamo [80, 78], in particular the role of the iron propellers and the possible influence of helicity in the propeller region [125]. A final explanation of the axisymmetric eigenmode and its comparably low critical Rm is, however, still missing.

5.5 The Bullard-von Kármán experiment in Lyon

A simple mechanical dynamo model, that had been proposed by Bullard in 1955, is the homopolar disk dynamo [22]: Imagine a metallic disk rotating with an angular velocity ω in a magnetic field \mathbf{B} . The emf $\mathbf{v} \times \mathbf{B}$ points from the axis to the rim of the disk and drives a current I through a wire that is wound around the axis of the disk. The orientation of the wire is such that the external magnetic field is amplified. At a critical value of ω , the amplification becomes infinite: self-excitation sets in. With growing magnetic field, the Lorentz force $\mathbf{j} \times \mathbf{B}$ acts against the driving torque, which will ultimately lead to saturation. The feasibility of such an experiment was recently discussed in a paper by Rädler and Rheinhardt [179].

Inspired by this disk dynamo, a team in Lyon has investigated an interesting experimental arrangement which generates a magnetic field by a simple trick [16]. Basically, it comprises a flow of the same $s_2^+t_2$ type as the VKS flow. The working fluid is, however, gallium instead of sodium ("von Kármán gallium" experiment, [250]). The magnetic Reynolds number reaches only values of 5 which is clearly not sufficient for dynamo action to occur. The trick is now that a part of the amplification process is taken over by an external electrical amplifier which takes as input the azimuthal field component measured by a Hall sensor and feeds a coil which produces an axial magnetic field. Roughly speaking, the Ω effect (i.e. the generation of a toroidal from a poloidal field by means of differential rotation) is produced by the flow, while the α effect is mimicked by the external amplifier. Very interesting results have been obtained with this machine, including intermittent reversals of the dipole field, as well as excursions [16].

5.6 Madison

At the University of Wisconsin, Madison, C. Forest and his colleagues have undertaken the "Madison dynamo experiment" (MDX) which is, in many respects, quite similar to the VKS dynamo. The flow topology is of the same $s_2^+t_2$ type with two counter-rotating toroidal eddies and two poloidal eddies which are pointing inward in the equatorial plane. Historically it is noteworthy that Winterberg had proposed exactly this propeller configuration as early as 1963 [256].

The difference to VKS is that MDX works not in a cylinder but in a 1 m diameter sphere (Figure 14) and that the flow is driven by two impellers with Kört nozzles instead of two disks (with blades) as in VKS. A lot of effort had been spent in the hydrodynamic and numerical optimization of the precise geometry of the $s_2^+t_2$ flow [54].

The MDX dynamo has not shown self-excitation up to present. It was a surprise, however, that the measured *induced* magnetic field turned out to be dominated by an axial dipole component (Figure 15), since such an induced axial dipole cannot be produced by a large scale axisymmetric flow [213].

Evidently, this puzzle has a striking resemblance with the self-excitation of the axisymmetric field in the VKS experiment. The most plausible explanation comes from assuming some sort of α effect in the flow. And again one has to bear in mind the extreme sensitivity of the mode selection to minor amounts of helical turbulence (i.e. α) in the impeller region that was identified (for VKS) in [125].

Further results have been published on intermittent bursts of dynamo action [157], the detailed measurement of the magnetic field structure [158], and its interpretation in terms of possible dynamo sources [214]. In the latter paper, the induction of an axial dipole has been interpreted as a sort of "turbulent diamagnetism", which is not necessarily in contradiction with the interpretation given in [125]. Present activities at MDX point on further optimizing the flow by installing various types of baffles.

Another focus of the Madison group is on replacing liquid metal experiments by plasma experiments. A main step in this direction is to confine the plasma and to drive a rotating flow by means of crossed magnetic and electric fields at the boundary [55, 40]. Interestingly, this is a configuration which had been used in many flow control experiments with low conducting fluids [63, 252]. The big advantage of plasma experiments is, of course, that Pm is not a constant of the material but can be adjusted in a wide range [251]. By controlling the poloidal profile of the toroidal rotation, high Rm flows will be generated that can result in MRI or dynamo action.

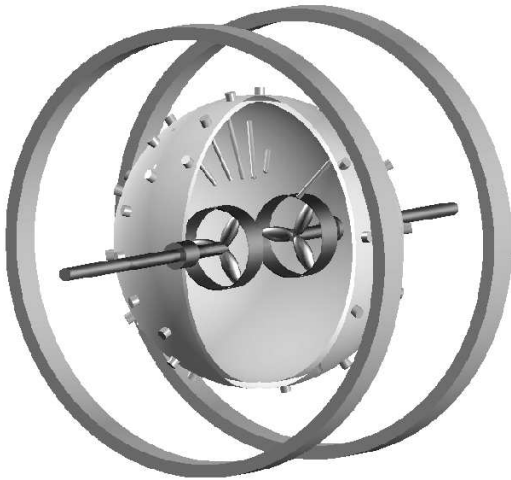


Fig. 14 Schematic plot of the Madison Dynamo experiment (MDX). The flow topology is of the same s_2+t_2 type as in the VKS experiment. The two rings symbolize the Helmholtz coil for producing an axial magnetic field. The lances for internal magnetic field sensors are also shown. Figure courtesy of E. Spence.

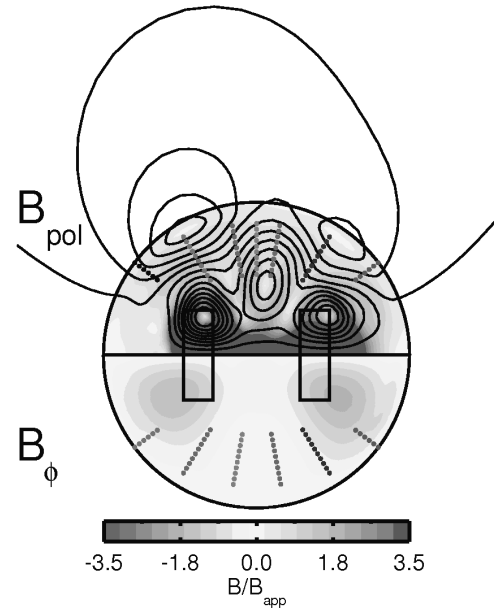


Fig. 15 Induced magnetic field structure measured in the MDX, including a significant axial dipole component. Figure courtesy of E. Spence.

5.7 The rotating torus experiment in Perm

An ingenious idea to circumvent the large driving power that is usually needed to do dynamo experiments has been pursued by the group of P. Frick at the Institute of Continuous Media Mechanics in Perm, Russia [56, 228, 43]. The idea relies on the fact that a helical flow of the Ponomarenko type can be produced within a torus when its rotation is abruptly braked and a fixed diverter forces the inertially continuing flow on a helical path. While this concept is very attractive not only with respect to the low motor power that is necessary to slowly accelerate the torus, but also with respect to the fact that the sodium can be perfectly confined in the torus without any need for complicated sealing, a less attractive feature is the non-stationarity of the flow allowing only the study of a transient growth and decay of a magnetic field.

Extensive water pre-experiments and numerical simulations [44] have been carried out to optimize and predict magnetic self-excitation in such a non-stationary dynamo. Figure (16) gives an impression of the flow that appears shortly after the braking of the torus. The major radius of the water-filled torus is 10 cm, the minor radius is 2.7 cm. The photograph was taken 1.5 s after the full stop.

Based on these preparations a sodium experiment has been build with the following dimensions: major radius of the torus 40 cm, minor radius of the torus 12 cm, mass of sodium 115 kg, rotation rate 3000 rpm, maximal velocity 140 m/s, effective magnetic Reynolds number 40, minimal braking time 0.1 s. The main problem for such an experiments is connected with the tremendous mechanical stresses that appear in the short braking period. A special bronze alloy has been used for of the torus. First water experiments have been carried out, but for a sodium experiment more safety tests will be necessary.

In the preparatory phase of this experiment, important results on mean-field turbulence parameter have been obtained with a smaller gallium experiment [228, 43]. The importance of these parameters results from the question whether highly turbulent flows with high Rm lead to an effective reduction of the conductivity of the liquid. This reduction has been described in the context of mean-field dynamo theory as β effect (cf. equation (11)). While a significant reduction by a factor $10^4 \dots 10^5$ can be well justified for the solar dynamo [113], the corresponding value for the geodynamo is not safely known. Recent studies of reversal sequences and their statistical properties suggest that the effective conductivity of the Earth's outer core might be reduced by a factor 3, when compared to the molecular conductivity of the material [52, 53]. Interestingly, this value is not that far from the factor 10 that was indicated by recent numerical simulations of mean-field coefficients in the geodynamo [203].

While neither the Riga nor the Karlsruhe dynamo experiment have shown any measurable β effect, there was only one experiment in which the measurement of an β effect had been claimed [185]. Now, the Perm group has identified, by means

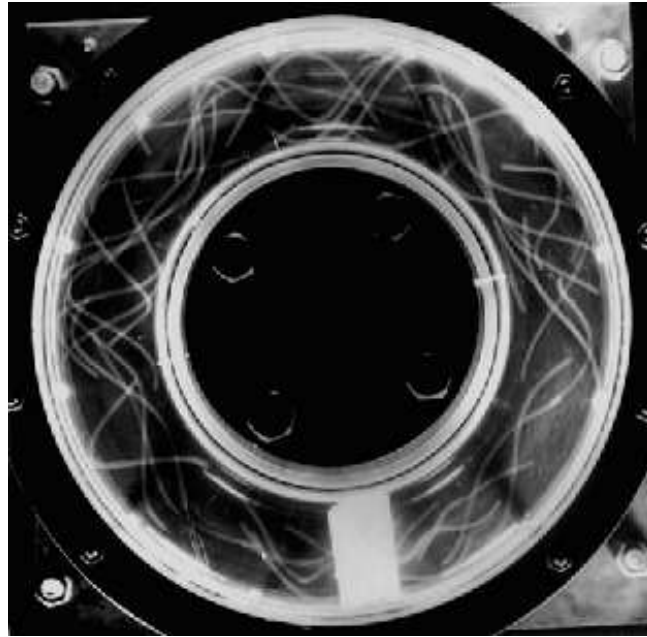


Fig. 16 Helical flow that develops after the abrupt brake of the torus in the Perm water test experiment, visualized by polystyrene particles. The white bar at the bottom of the picture represents the diverter. Figure courtesy of P. Frick.

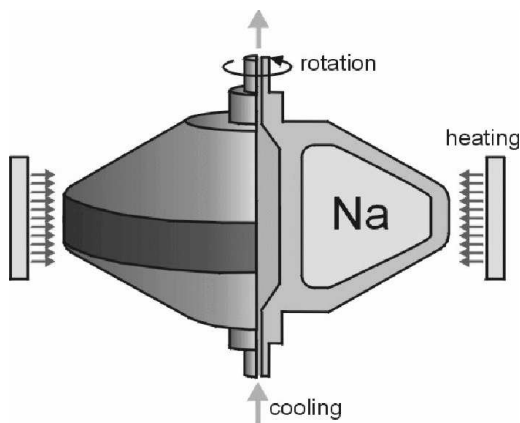


Fig. 17 The first dynamo experiment in Maryland. A rapidly rotating torus is heated at the rim and cooled at the axis. Figure courtesy of D. Lathrop.

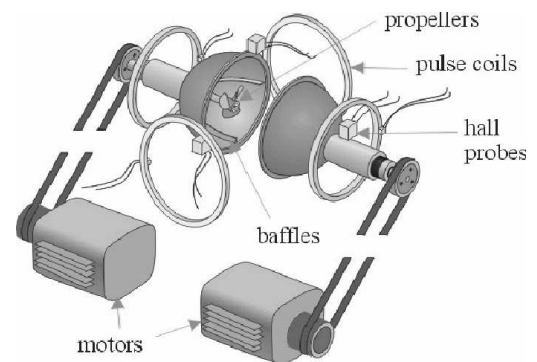


Fig. 18 The second dynamo experiment in Maryland. In a 0.3 m diameter sphere different flows have been produced by propellers. This configuration, but with the propellers replaced by an inner sphere, was used for the MRI experiment. Figure courtesy of D. Lathrop.

of a very thorough measurement technique, a conductivity reduction in the order of 1 per cent for a comparably low Rm of ≈ 1 [43]. This sounds not very much, but since the dependence of β on Rm starts to be quadratic (in the low-conductivity limit) one could well imagine a significant β effect in planetary core flows characterized by much higher values of Rm .

5.8 Sodium experiments in Maryland

A variety of liquid sodium experiments have been carried out under the guidance of D. Lathrop at the University of Maryland [162, 163, 128, 205, 210, 211, 206].

In the first experiment (Dynamo I, see Figure 17), a 0.2 m diameter titanium vessel containing 1.5 l of liquid sodium was heated on the outer side and cooled at the axis. The fast rotation (up to 25000 rpm!) was intended to induce centrifugally driven convection, with the centrifugal force as a substitute for gravitation in the planetary case. Self-excitation was not observed.

The second device (Dynamo II, see Figure 18) consisted of a 0.3 m diameter sphere made of steel. A total of 15 l of sodium was stirred by two counter-rotating propellers, each powered by 7.4 kW motors. Note that the flow is again of the $s_2^+t_2$ topology as in VKS and MDX. The most interesting result of this experiment was obtained by carefully analyzing

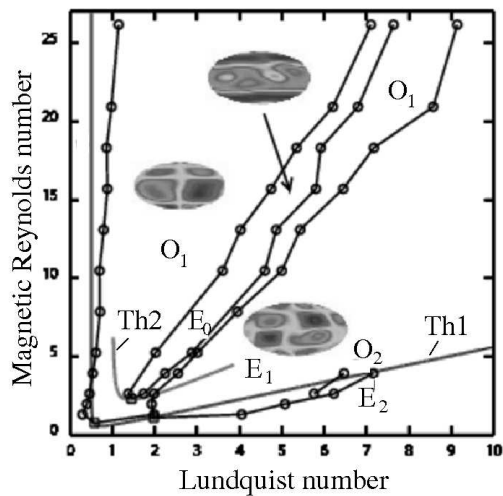


Fig. 19 Phase diagram of the spherical Couette experiment in dependence on the Lundquist number and the magnetic Reynolds number. O_1 , E_1 , O_2 AND e_2 are different modes. Th_1 and Th_2 are the theoretical stability boundary curves from the dispersion relation for the longest (Th_1) and second longest wavelength. Figure courtesy of D. Lathrop.

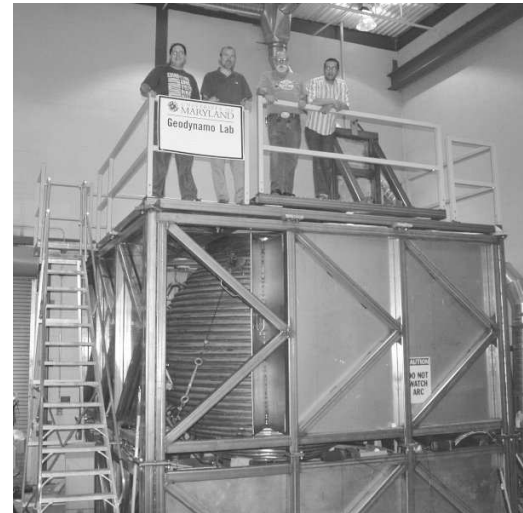


Fig. 20 The rotating 3m sphere in Maryland. An impressive video is available under www.youtube.com. Figure courtesy of D. Lathrop.

the decay rates of different modes. The decay of an axisymmetric applied field turned out to be more slowly as Rm was increased, while the decay of a non-axisymmetric field even accelerated with increasing Rm . Actually the decrease of the decay rate of the axisymmetric magnetic field was by about 30 per cent compared to the un-stirred fluid, at a magnetic Reynolds number of about 65. Naively, a simple extrapolation of this trend would point to a critical Rm of around 200. Although we know from Cowling's theorem how problematic an interpolation of decay rates of an axisymmetric mode towards zero is [242], one might ask again if not a similar mechanism as in VKS (and MDX) could provide a positive growth rate of an axisymmetric field.

Maybe the most important result of the Maryland group was obtained with a modification of this Dynamo II. By replacing the two propellers by one 5 cm diameter sphere, one arrives at a classical spherical Couette configuration. Applying, as before, an axial magnetic field to this flow, new modes of correlated magnetic field and velocity perturbation appeared [211] in certain parameter regions of Rm and S (see Figure 19). On closer inspection the dependence of these modes on Rm and S turned out to be in amazingly accurate correspondence with predictions of the MRI based on the dispersion relations. Running in an already strongly turbulent regime, this experiment was certainly not able to show MRI as the *first instability of a stable flow*. Nevertheless, it is tempting to speculate (in the spirit of [134]) that the fine-grained background turbulence just gives some renormalized viscosity, without terribly affecting the basic mechanism of MRI that seems robust enough to show up as an "coherent structure" as long as only Rm and S are in the right range.

The most recent project of the Maryland group is the construction of a giant rotating sphere with 3 m diameter (Figure 20), for future studies of MHD instabilities and (hopefully) the dynamo effect in rotating systems.

5.9 Grenoble

Continuing the tradition of former geophysically inspired experiments [20, 3], a group in Grenoble has prepared the so-called DTS ("Derviche Tourneur Sodium") experiment which is quite similar to the MRI experiment in Maryland. The distinguishing feature is a permanent magnet in the inner sphere in order to study the magnetostrophic regime [28] even when self-excitation is expectedly not achieved (Figure 21).

One of the most important results of the DTS experiment was the experimental observation of strong super-rotation of the liquid sodium in the equatorial region [153], which had been predicted by Dormy et al. in 1998 [45]. This was made possible by inferring velocity profiles from electric potentials measurements at the rim of the spherical container. While the observed latitudinal variation of the electric potentials in the experiments differs markedly from the predictions of a numerical model similar to that of Dormy, recent numerical results show a better agreement with the measurements [93].

A further focus of the DTS experiment is the investigation of various wave phenomena in magnetized rotating flows [201].

5.10 Princeton

A group at Princeton Plasma Physics Laboratory, headed by H. Ji, has a long tradition in doing plasma experiments with relevance to astrophysical processes, in particular to magnetic reconnection [98] and the α effect [99] (which is, in the laboratory fusion plasma community, sometimes denoted as "dynamo effect" [14]).

At present an experiment is under preparation that is intended to show MRI in a Taylor-Couette cell filled with liquid gallium, at Reynolds numbers of several millions [100]. The basic question for such an experiment is, of course, under which conditions the underlying flow can really be considered laminar. Although Rayleigh's criterion predicts linear stability for the ratio of rotation rates of outer to inner cylinder being larger than the squared ratio of inner to outer radius, it has long been thought that the effect of boundaries together with non-linear instabilities will make the flow ultimately turbulent. Actually, in the linear stable regime turbulence had been reported by a number of authors [253, 200, 46].

After a long optimization process [102], the Princeton group has finally succeeded to find such a configuration of differentially rotating end rings that preserves the Taylor-Couette profile of the angular velocity. The measured torques, fluctuation levels and Reynolds stresses suggest that the flow is indeed laminar up to Reynolds numbers of about 2×10^6 [101]. Experiments with liquid gallium are presently under preparation. Recent numerical simulations suggest that the MRI should indeed be identifiable in such an experiment, in particular by its linear growth and the increased torque [137].

However, as usual for such experiments, some uncertainties remain. They concern, in particular, the not well understood role of the rotating rings in the end-caps. Actually, the rotation rates which have been chosen in the experiment in order to restore the Taylor-Couette flow profile are different from the numerically optimized ones. To explain this discrepancy, even cylinder wobbling has been invoked, which may point to a quite complicated process involved in restoring the Taylor-Couette profile [187, 137].

On the other hand, the Maryland experiment has shown that MRI seems to be a quite robust phenomenon that appears quite independently on other flow features as long as only the necessary combination of Rm and S is reached.

However this might be, the Princeton gallium experiment will certainly teach us a lot about hydromagnetic instabilities in Taylor-Couette flows at high Rm .

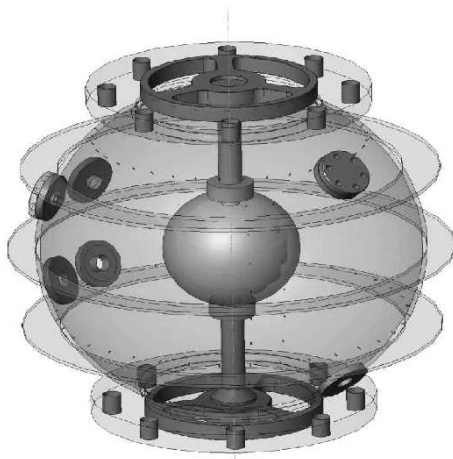


Fig. 21 The DTS experiment in Grenoble. Forty liters of liquid sodium are contained between a 7.4 cm inner sphere and a 21 cm radius outer sphere. The copper inner sphere contains a magnet which produces a nearly dipolar field with a maximum of 0.345 T in fluid close to the poles. Figure courtesy of D. Schmitt and the DTS team.

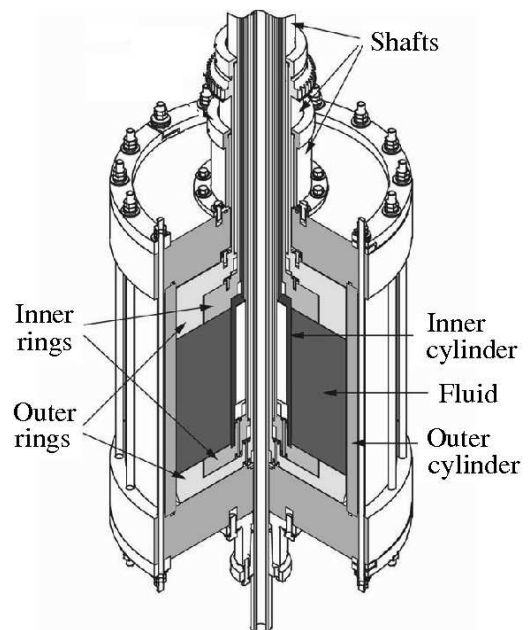


Fig. 22 The Princeton MRI experiment. The rotating gallium of height 27.86 cm is contained between two differentially rotating concentric cylinders of radii 7.06 cm and 20.30 cm. Figure courtesy of H. Ji.

5.11 The sodium experiment in New Mexico

Since a couple of years, a sodium experiment is under construction at the New Mexico Institute of Mining and Technology (NMIMT) in Socorro [37, 38]. The title of the project is "The $\alpha - \Omega$ accretion disk dynamo that powers active galactic nuclei (AGN) and creates the magnetic field of the universe."

At the present stage, the experiment is a Taylor-Couette experiment (Figure 23), quite similar to the Princeton experiment. It is planned to produce an α effect by means of "plumes" that are driven by pulsed jets. The envisioned Rm , based on the rotation alone, is 130, the corresponding Rm for the plumes is 15 [37]. The water experiments have already revealed that the differential rotation of the Couette flow speeds up the anticyclonic rotation of the plumes. This anticyclonic rotation will form the basis for the α -effect of the α - Ω -dynamo.

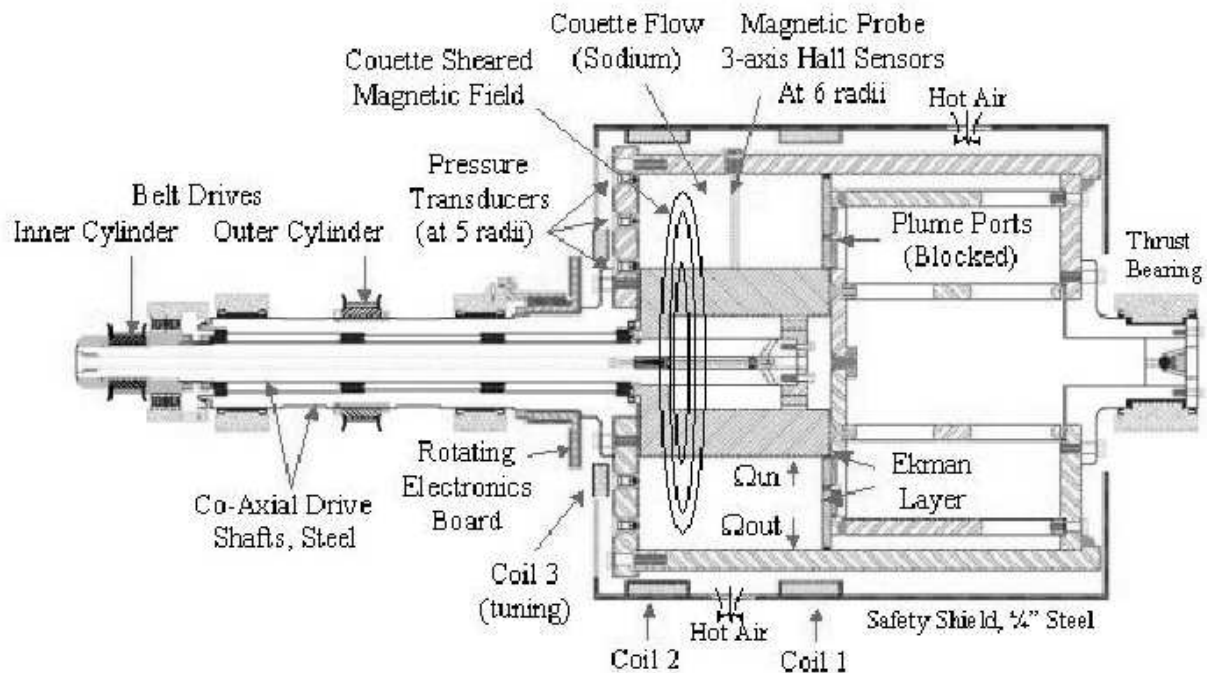


Fig. 23 The NMIMT $\alpha - \Omega$ experiment, at the present stage without the pulsed jet. Figure courtesy of S. Colgate.

5.12 The MRI experiment in Obninsk

An MRI experiment with liquid sodium, proposed by E.P. Velikhov, is under preparation at the Institute of Physics and Power Engineering in Obninsk (Russia), in collaboration with the Kurchatov Institute in Moscow. The basic idea is to drive a flow in a torus of rectangular cross-section by a Lorentz force due to an applied vertical field and an applied radial current [248, 108, 109]. The hope is that in the bulk of the volume one gets an angular velocity dependence $\sim r^{-2}$ which would exactly correspond to the Rayleigh line. A similar experiment had been proposed in [229], although as a Taylor-Dean flow to have the angular momentum increasing at all radii. While experimental results are not available from those experiments an interesting claim has been made on a re-interpretation of the Moresco-Alboussiere experiment [147, 118] on the stability of the Hartmann flow in terms of MRI [110].

5.13 The PROMISE experiment in Dresden-Rossendorf

In this last subsection we leave the realm of high Rm flows and discuss an experiment on a particular type of MRI which has been coined "inductionless MRI" [173] or "helical MRI" (HMRI) [136].

The background for this is the following: We have seen, in connection with "standard MRI" (SMRI) experiments with an axially applied magnetic field, that it is extremely difficult to keep those high Re flows laminar. However, those high Re are not a genuine necessity for MRI, but just a consequence of the need for Rm in the order of one or larger.

The reason for this is that the azimuthal magnetic field (which is an unavoidable ingredient for MRI) must be *induced* from the applied axial field by the rotation of the flow, and such induction effects are just proportional to Rm . This being said, one could ask why not to replace the induction process by just *externally applying* the azimuthal magnetic field as well? This question was addressed in a 2005 paper by Hollerbach and Rüdiger [92], who showed that the MRI is then possible with dramatically reduced experimental effort. Actually, the scaling characteristics of this HMRI are completely

different from those of SMRI. While the latter needs Rm and S of the order of 1, the former depends on Re and Ha (or the interaction parameter N).

HMRI is currently the subject of intense discussions in the literature [165, 194, 135, 136, 173, 235, 236, 126], the roots of which trace back to an early dispute between Knobloch [115] and Hawley and Balbus [8].

A remarkable property of HMRI, which has been clearly worked out in [173], is the apparent paradox that a magnetic field triggers an instability though the dissipation is larger than without magnetic fields. This is not so surprising when put in the context of other *dissipation induced instabilities* which are quite common in many areas [121, 112].

Another, and not completely resolved, issue concerns the relevance of HMRI for astrophysical flows. On first glance, HMRI seems well capable to work in cold regions of accretion disks characterized by small Pm where SMRI cannot work. This scenario might indeed be important for the "dead zones" of protoplanetary disks [245] as well as for the outer parts of accretion disks around black holes [10].

However, before entering such a discussion in detail, one has to check whether HMRI works at all for Keplerian rotation profiles $\Omega(r) \sim r^{-3/2}$. While the answer resulting from the dispersion relation was negative [135], the solution of the eigenvalue equation gave an affirmative answer, as long as at least the outer or the inner radial boundary is conducting [195].

Unfortunately, even this is not the end of the story. Since HMRI appears in the form of a travelling wave, one has to be quite careful with the interpretation of the instability of a single monochromatic wave. Actually, one has to look for wave packet solutions with vanishing group velocity. Typically, the regions in parameter space for this *absolute instability* are only a subset of those for the *convective instability*. A comprehensive analysis of this topic is under preparation [174].

Notwithstanding this ongoing discussion, the dramatic decrease of the critical Re and Ha for the onset of the MRI in helical magnetic fields, as compared with the case of a purely axial field, made this new type of MRI very attractive for experimental studies.

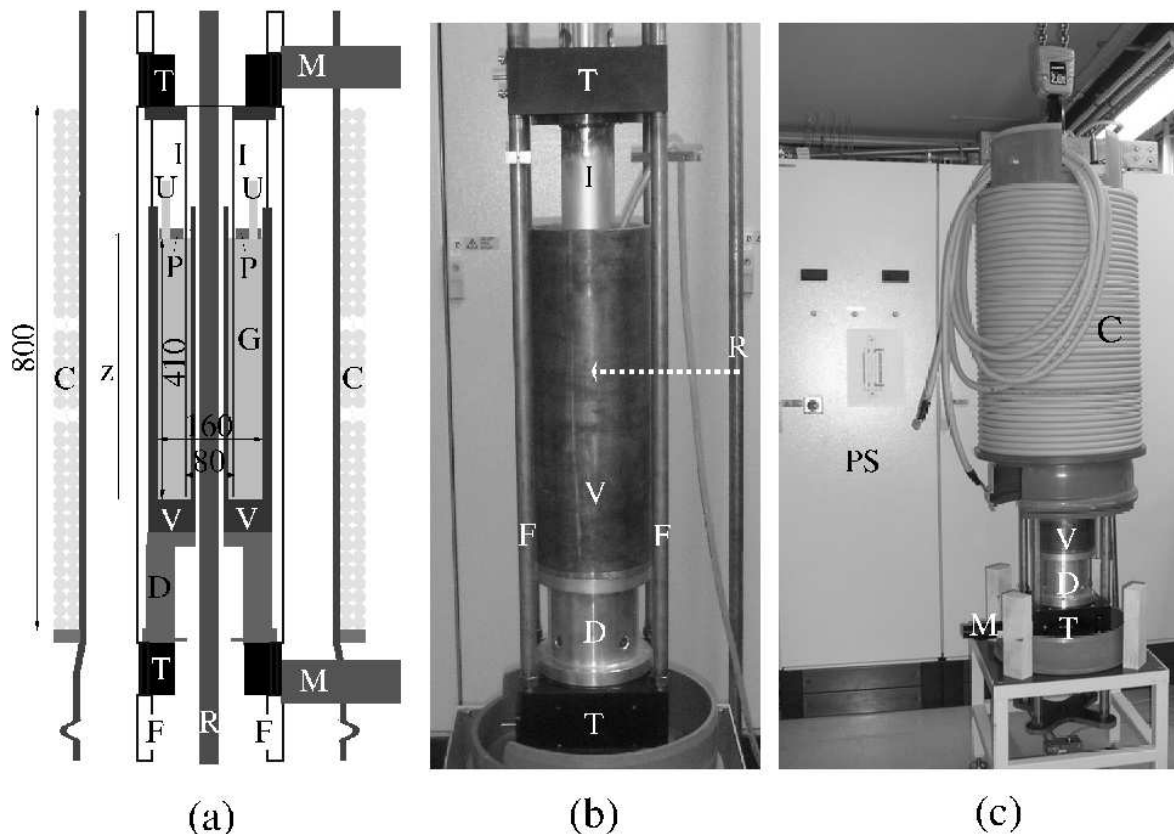


Fig. 24 The PROMISE experiment. (a) Sketch. (b) - Photograph of the central part. (c) - Total view with the coil being installed. V - Copper vessel, I - Inner cylinder, G - GaInSn, U - Two ultrasonic transducers, P - Plexiglas lid, T - High precision turntables, M - Motors, F - Frame, C - Coil, R - Copper rod, PS - Power supply for currents up to 8000 A. The indicated dimensions are in mm.

The PROMISE facility (*Potsdam ROssendorf Magnetic InStability Experiment*), shown in Figure 24, is basically a cylindrical Taylor-Couette cell with externally imposed axial and azimuthal magnetic fields. Its primary component is a

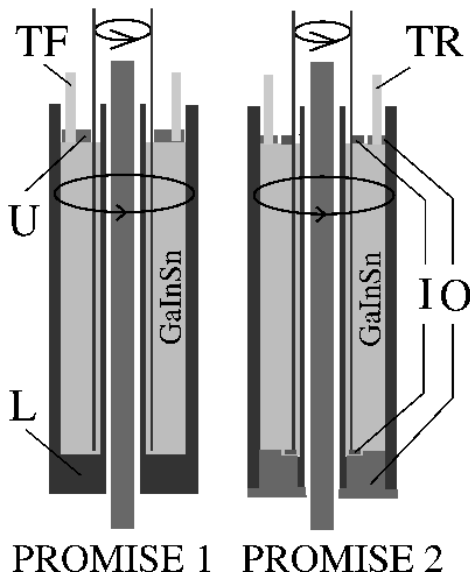


Fig. 25 The asymmetric end cap configuration in PROMISE 1 is replaced by a symmetric one in PROMISE 2. U - Upper end cap fixed in the laboratory frame, L - Lower end cap, made of copper, rotating with the outer cylinder, I - Inner plastic rings, O - Outer plastic rings, TF - Fixed ultrasonic transducer, TR - Rotating ultrasonic transducer.

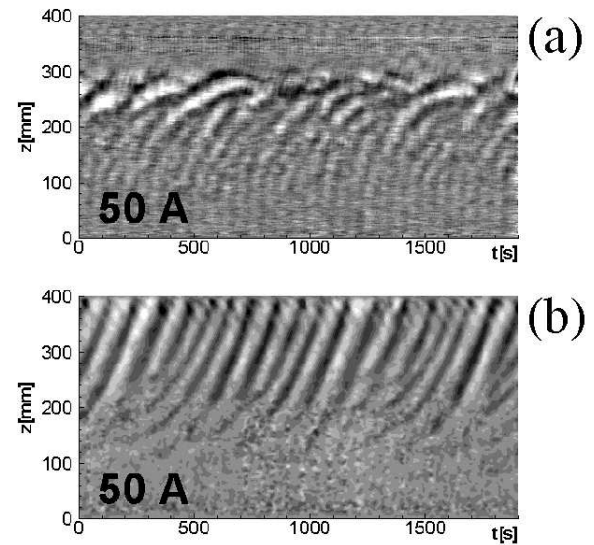


Fig. 26 The measured axial velocity perturbation for $Re = 2975$ and $I_{coil} = 50$ A, showing the appearance of MRI as a travelling wave. (a) PROMISE 1 experiment with $I_{rod} = 6000$ A. (b) PROMISE 2 experiment with $I_{rod} = 7000$ A.

cylindrical copper vessel V, fixed on a precision turntable T via an aluminum spacer D. The inner wall of this vessel is 10 mm thick, extending in radius from 22 to 32 mm; the outer wall is 15 mm thick, extending from 80 to 95 mm. The outer wall of this vessel forms the outer cylinder of the TC cell. The inner cylinder I, also made of copper, is fixed on an upper turntable, and is then immersed into the liquid metal from above. It is 4 mm thick, extending in radius from 36 to 40 mm, leaving a 4 mm gap between it and the inner wall of the containment vessel V. The actual TC cell therefore extends in radius from 40 to 80 mm, for a gap width $d = r_o - r_i = 40$ mm. This amounts to a radius ratio of $\eta := r_i/r_o = 0.5$. The fluid is filled to a height of 400 mm, for an aspect ratio of ~ 10 . Axial fields of the order of 10 mT are produced by a coil C, and azimuthal fields of the same order are produced by currents of up to 8000 A in a water cooled copper rod R going through the center of the facility.

First results of PROMISE were published recently [225, 197, 226]. The most important result was the appearance of MRI in form of a travelling wave in a limited window of Ha (which is proportional to the coil current I_{coil}). The frequency of this wave turned out to be in good agreement with numerical predictions.

The intricacies of this PROMISE 1 experiment, as we call it now, trace back to the two points discussed above. First, HMRI only slightly extends beyond the Rayleigh line and, second, the small unstable region for the convective instability is further reduced when considering the absolute instability. From this high sensitivity of the instability with respect to $\mu := \Omega_o/\Omega_i$ one has to be careful with Ekman/Hartmann pumping and a possible change of the profiles by short circuited currents which can drive a Dean flow [236]. Another point is the critical role of the radial jet approximately at mid-height of the Taylor-Couette cell at which the MRI wave is typically stopped [227]. This radial jet results from the Ekman pumping at the lower and upper end caps.

For all those reasons, some changes of the axial boundary conditions have been implemented in a modified experiment which is called now PROMISE 2. As suggested by a thorough analysis of Szklarski [236], the Ekman pumping can be minimized by using split rings, the inner one rotating with the inner cylinder and the outer rotating with the outer cylinder, with a splitting position at 0.4 of the gap width (Figure 25). Both upper and lower rings are now made of insulating material. Since the ultrasonic transducers are rotating with the outer ring (i.e. with the slow rotation rate of the outer cylinder) their signal must be transmitted by slip rings to the computer.

Without going into the detailed results of the PROMISE 2 experiment, which will be published elsewhere, we can state that these modifications bring about a drastic improvement of the MRI wave and a significant sharpening of the transitions between stable and unstable regimes. In Figure 26 we see that for PROMISE 2 the MRI wave goes through the entire volume while it was stopped at the radial jet position in PROMISE 1.

6 Conclusions and prospects

The last ten years have seen tremendous progress in liquid metal experiments on the origin and the action of cosmic magnetic fields. With the success of the complementary sodium experiments in Riga and Karlsruhe in 1999 it was shown that self-excitation works not only in computer programs on the basis of rather smooth flows, but also in real-world turbulent flows. Kinematic dynamo theory has been shown to be robust with respect to low levels of turbulence and complicated boundary and interface conditions. The saturation mechanism in the Riga experiment is non-trivial as it results not only from a global pressure increase but also from a significant redistribution of the flow.

While the Riga and Karlsruhe dynamos are characterized by an amazing predictability, in some respect one can learn even more from the efforts to make the VKS dynamo (and also the MDX dynamo) running. After some modifications of the original concept, the VKS experiment was eventually successful in self-exciting a magnetic field. The fact that the observed eigenfield in VKS is essentially an axisymmetric dipole, in contrast to the original prediction of an equatorial dipole, is an inspiring challenge to understand better the intricate field amplification loop the dynamo mechanism relies on. The "little brother" of the VKS experiment, the VKG experiment in Lyon, has yielded fascinating field reversals when complemented by an external amplification loop that mimics a sort of α effect.

On the way to the final rotating torus experiment, the Perm group has obtained important results concerning the mean-field coefficients in turbulent flows.

After dynamo action has thus been proven, one observes presently some tendency to take a breath and turn back to somewhat smaller machines in order to study MHD instabilities and wave phenomena. The identification of the MRI is only one aspect in this direction, though an important one due to the enormous astrophysical implications of this instability. Apart from standard MRI (Maryland, Princeton, New Mexico) and helical MRI (Dresden-Rosendorf) there are other magnetic instabilities that are capable of destabilizing hydrodynamically stable flows or even fluids at rest. Among them we have to note the Taylor-Vandakurov instability (with a current flowing through the liquid) [246, 237, 215] and the "azimuthal MRI" (AMRI) [196] based on an purely azimuthal field. Future experiments on those instabilities are very desirable.

There are many wave phenomena in rotating fluids under the influence of (externally applied or self-excited) magnetic fields which still deserve a deeper understanding. At this point we observe a revival of the activities in the sixties on Alfvén wave studies with liquid metals. In this respect, it might also be interesting that presently magnetic fields are available [258] which are so strong that for potassium and sodium the Alfvén velocity exceeds the sound velocity. The small scale experiments in Maryland and Grenoble have provided a wealth of data, and the 3 m sphere in Maryland will be a fascinating tool for extending those investigations into extreme parameter regions.

An interesting direction of future research could be the experimental investigation of precession driven dynamos, for which a water test experiment had been carried out by Léorat et al. [132, 133]. Numerical work by Tilgner [244] points to a critical Rm of around 200 which makes a laboratory experiments not unrealistic. Of course, much more optimization would be necessary before such an experiment could be designed.

If one had a wish for free, one could think of constructing a huge self-sustaining nonlinear dynamo [186] (or "self-creating dynamo" [57]). One could start, for example, in the hydrodynamic stable regime of a Taylor-Couette flow (mimicking a Keplerian flow) which could be destabilized, via MRI, by an externally applied magnetic field. Suppose now that the resulting flow would act as a dynamo, the resulting eigenfield could possibly replace the initially applied magnetic field as a trigger for the instability.

Having another wish for free, one could also think about the experimental realization of a fluctuation dynamo, based on more or less homogeneous isotropic turbulence [199]. For those flows, critical Rm around 200 have been found in recent simulations. However, simple Kolmogorov scaling arguments tell us that such a "James-Bond-dynamo" ("...shaken, not stirred...") is only possible with a giant input power of many Megawatts.

In spite of the fact that liquid metal experiments should not be expected to be perfect Bonsai models of any real astrophysical systems, experimental work has already started to change some views on those natural systems. Maybe that the Riga dynamo will once become a model of the double helix nebula close to the galactic center [148, 207], maybe that the partitioning of α and Ω effects in the VKS dynamo will re-animate the old Babcock-Leighton theory of the solar dynamo [6], maybe that the PROMISE experiment will illuminate the possible action of helical MRI in cold parts of accretion disks where standard MRI cannot work.

Acknowledgements Support from Deutsche Forschungsgemeinschaft in the framework of SFB 609, from European Commission under contract 028679, and from Leibniz-Gemeinschaft in the framework of the SAW project PROMISE is gratefully acknowledged. We are indebted to Raul Avalos-Zuñiga, Michael Christen, André Giesecke, Thomas Gundrum, Uwe Günther, Rainer Hollerbach, Saša Kenjereš, Jacques Léorat, Olgerts Lielausis, Ernests Platācis, Jānis Priede, Karl-Heinz Rädler, Günther Rüdiger, Luca Sorriso-Valvo, Jacek Szklarski, and Mingtian Xu for the fruitful collaboration over the course of many years.

References

- [1] A. Alemany, Ph. Marty, F. Plunian, and J. Soto, *J. Fluid Mech.* **403**, 262–276 (2000).
- [2] Aristotle, *De anima (On the soul)* (Penguin, Harmondsworth, 1986), pp. 135–136.
- [3] J. Aubert, D. Brito, H.-C. Nataf, P. Cardin, and J.-P. Masson, *Phys. Earth Planet. Inter.* **128**, 51–74 (2001).
- [4] J. Aubert, J. Aurnou, and J. Wicht, *Geophys. J. Int.* **172**, 945–956 (2008).
- [5] R. Avalos-Zuñiga, M. Xu, F. Stefani, G. Gerbeth, and F. Plunian, *Geophys. Astrophys. Fluid Dyn.* **101**, 389–403 (2007).
- [6] H.W. Babcock, *Astrophys. J.* **133**, 572 (1961).
- [7] S.A. Balbus and J. F. Hawley, *Astrophys. J.* **376**, 214–222 (1991).
- [8] J.F. Hawley and S.A. Balbus, *Astrophys. J.* **400**, 595–609 (1992).
- [9] S.A. Balbus and J. F. Hawley, *Rev. Mod. Phys.* **70**, 1–53 (1998).
- [10] S.A. Balbus and P. Henri, *Astrophys. J.* **674**, 408–414 (2008).
- [11] R. Beck, A. Brandenburg, D. Moss, A. Shukurov, and D. Sokoloff, *Ann. Rev. Astron. Astrophys.* **34**, 155–206 (1996).
- [12] M. Berhanu et al., *EPL* **77**, 59001 (2007).
- [13] M.K. Bevir, *J. Br. Nucl. Energy Soc.* **12**, 455–458 (1973).
- [14] E.G. Blackman and H. Ji, *Mon. Not. R. Astron. Soc.* **369**, 1837–1848 (2006).
- [15] M. Bourgoin et al., *Phys. Fluids* **14**, 3046–3058 (2001).
- [16] M. Bourgoin et al., *New J. Phys.* **8**, 329 (2006).
- [17] J. Braithwaite and H.C. Spruit, *Nature* **431**, 819–821 (2004).
- [18] A. Brandenburg and K. Subramanian, *Phys. Rep.* **417**, 1–209 (2005).
- [19] A. Brandenburg, K.-H. Rädler, and M. Schrunner, *Astron. Astrophys.* **482**, 739–746 (2008).
- [20] D. Brito, P. Cardin, H.-C. Nataf, and G. Marolleau, *Phys. Earth Planet. Inter.* **91**, 77–98 (1995).
- [21] B. Brunhes, *J. Phys.* **5**, 705–724 (1906).
- [22] E.C. Bullard, *Proc. Camb. Phil. Soc.* **51**, 744–760 (1955).
- [23] F.H. Busse, *Geophys. J. R. Astr. Soc.* **42**, 437–459 (1975).
- [24] F.H. Busse, *Ann. Rev. Fluid Mech.* **10**, 435–462 (1978).
- [25] F.H. Busse, *Annu. Rev. Fluid Mech.* **31**, 383–408 (2000).
- [26] F.H. Busse, *Phys. Fluids* **14**, 1301–1314 (2002).
- [27] F.H. Busse, E. Grote, and A. Tilgner, *Stud. Geophys. Geod.* **42**, 1–6 (1998).
- [28] P. Cardin, D. Brito, D. Jault, H.-C. Nataf, and J.-P. Masson, *Magnetohydrodynamics* **38**, 177–189 (2002).
- [29] J.B. Carlson, *Science* **189**, 753–760 (1975).
- [30] S. Chandrasekhar, *Proc. Nat. Acad. Sci.* **46**, 253–257 (1960).
- [31] S. Childress, and A. D. Gilbert, *Stretch, Twist, Fold: The Fast Dynamo* (Springer, Berlin/Heidelberg/New York, 1995).
- [32] M. Christen, H. Hänel, and G. Will, in *Beiträge zu Fluidenergiemaschinen 4*, edited by W. H. Faragallah and G. Grabow (Faragallah-Verlag und Bildarchiv, Sulzbach/Ts., 1998), pp. 111–119.
- [33] U.R. Christensen, P. Olson, and G. A. Glatzmaier, *Geophys. J. Int.* **138**, 393–409 (1999).
- [34] U.R. Christensen and A. Tilgner, *Nature* **429**, 169–171 (2004).
- [35] U.R. Christensen, *Nature* **444**, 1056–1058 (2006).
- [36] U.R. Christensen and J. Aubert, *Geophys. J. Int.* **166**, 97–114 (2006).
- [37] S.A. Colgate, H. Li, and V. Pariev, *Phys. Plasmas* **8**, 2425–2431 (2001).
- [38] S.A. Colgate et al., *Magnetohydrodynamics* **38**, 129–142 (2002).
- [39] S.A. Colgate, *Astron. Nachr.* **327**, 456–460 (2006).
- [40] C. Collins, C.B. Forest, R. Kendrick, and A. Seltzman, *Bull. Amer. Phys. Soc.* **52**, No. 11, BP8.00113 (2007).
- [41] J.E.P. Connerney, M. H. Acuña, P. J. Wasilewski, G. Kletetschka, N. F. Ness, H. Rème, R. P. Lin, and D. L. Mitchell, *Geophys. Res. Lett.* **28**, 4015–4018 (2001).
- [42] T.G. Cowling, *Mon. Not. Roy. Astr. Soc.* **140**, 39–48 (1934).
- [43] S.A. Denisov, V.I. Noskov, R.A. Stepanov, and P.G. Frick, *JETP Letters* **88**, 167–171 (2008).
- [44] W. Dobler, P. Frick, and R. Stepanov, *Phys. Rev. E* **67**, 056309 (2003).
- [45] E. Dormy, P. Cardin, and D. Jault, *Earth Planet. Sci. Lett.* **160**, 15–30 (1998).
- [46] B. Dubrulle et al., *Phys. Fluids* **17**, 095103 (2005).
- [47] M.L. Dudley and R. W. James, *Proc. R. Soc. Lond.* **A425**, 407–429 (1989).
- [48] N. Dziourkevitch, D. Elstner, and G. Rüdiger, *Astron. Astrophys.* **423**, L29–L32 (2004).
- [49] S. Fauve and F. Petrelis, *C.R. Phys.* **8**, 87–92 (2007).
- [50] D.R. Fearn, *Rep. Prog. Phys.* **61**, 175–235 (1998).
- [51] D.R. Fearn, P.H. Roberts, and A.M. Soward, in *Energy, Stability, and Convection*, edited by G. P. Galdi and B. Straughan (Longmans, New York, 1988), pp. 60–324.
- [52] M. Fischer, F. Stefani, and G. Gerbeth, *Eur. J. Phys. B*, in press (2008); arxiv.org/0709.3932.
- [53] M. Fischer, G. Gerbeth, A. Giesecke, and F. Stefani, *Inverse Problems*, submitted (2008); arxiv.org/0808.3310.
- [54] C.B. Forest et al., *Magnetohydrodynamics* **38**, 107–120 (2002).
- [55] C.B. Forest et al., *Bull. Amer. Phys. Soc.* **52**, No. 11, BP8.00114 (2007).
- [56] P. Frick et al., *Magnetohydrodynamics* **38**, 143–162 (2002).
- [57] H. Fuchs, K.-H. Rädler, M. Rheinhardt, *Astron. Nachr.* **320**, 129–133 (1999).
- [58] A. Gailitis, *Magnetohydrodynamics* **3**, No. 3, 23–29 (1967).
- [59] A. Gailitis, *Magnetohydrodynamics* **32**, 58–62 (1996).
- [60] A. Gailitis and Ya. Freibergs, *Magnetohydrodynamics* **12**, 127–129 (1976).

- [61] A. Gailitis and Ya. Freibergs, *Magnetohydrodynamics* **16**, 116–121 (1980).
- [62] A.K. Gailitis et al., *Magnetohydrodynamics* **23**, 349–353 (1987).
- [63] A. Gailitis, *Appl. Magnetohydrodyn.* **12**, 143 (1961).
- [64] A. Gailitis et al., *Phys. Rev. Lett.* **84**, 4365–4368 (2000).
- [65] A. Gailitis et al., *Phys. Rev. Lett.* **86**, 3024–3027 (2001).
- [66] A. Gailitis, O. Lielausis, E. Platācis, G. Gerbeth, and F. Stefani, *Magnetohydrodynamics* **37**, No. 1/2, 71–79 (2001).
- [67] A. Gailitis et al., *Magnetohydrodynamics* **38**, 5–14 (2002).
- [68] A. Gailitis, O. Lielausis, E. Platācis, G. Gerbeth, and F. Stefani, *Magnetohydrodynamics* **38**, 15–26 (2002).
- [69] A. Gailitis, O. Lielausis, E. Platācis, G. Gerbeth, and F. Stefani, *Rev. Mod. Phys.* **74**, 973–990 (2002).
- [70] A. Gailitis, O. Lielausis, E. Platācis, G. Gerbeth, and F. Stefani, *Surv Geophys.* **24**, 247–267 (2003).
- [71] A. Gailitis, O. Lielausis, E. Platācis, G. Gerbeth, and F. Stefani, *Phys. Plasmas* **11**, 2838–2843 (2004).
- [72] A. Gailitis, O. Lielausis, G. Gerbeth, and F. Stefani, in: *Magnetohydrodynamics: Historical Evolution and Trends*, edited by S. Molokov, R. Moreau, H.K. Moffatt (Springer, Dordrecht, 2007), pp. 37–54.
- [73] A. Gailitis, G. Gerbeth, Th. Gundrum, O. Lielausis, E. Platācis, and F. Stefani, *C.R. Phys.* **9**, 721–728 (2008).
- [74] R.F. Gans, *J. Fluid Mech.* **45**, 111–130 (1970).
- [75] W. Gekelman, *J. Geophys. Res.* **104** 14417–14435 (1999)
- [76] H. Gellibrand, H., *A discourse mathematical on the variation of the magneticall needle*, reprint edited by G. Hellmann (A. Asher, Berlin, 1887).
- [77] A. Giesecke, U. Ziegler, and G. Rüdiger, *Phys. Earth Planet. Inter.* **152**, 90–102 (2005).
- [78] A. Giesecke, F. Stefani, and G. Gerbeth, *Magnetohydrodynamics*, in press (2008); arXiv:0803.3261.
- [79] W. Gilbert, *De Magnete*, translated by P. F. Mottelay, (Dover, New York, 1958).
- [80] C. Gissinger, A. Iskakov, S. Fauve, and E. Dormy, *EPL* **82**, 29001 (2008).
- [81] K.-H. Glassmeier et al., *Space Sci. Rev.* **132**, 511–527 (2007).
- [82] K.-H. Glassmeier, H.U. Auster, and U. Motschmann, *Geophys. Res. Lett.* **34**, L22201 (2007).
- [83] G.A. Glatzmaier and P. H. Roberts, *Nature* **377**, 203–209 (1995).
- [84] F. Govoni and L. Feretti, *Int. J. Mod. Phys. D* **13**, 1549–1594 (2004).
- [85] D. Grasso and H. R. Rubinstein, *Phys. Rep.* **348**, 163–266 (2001).
- [86] J.-L. Guermond, R. Laguerre, J. Léorat, and C. Nore, *J. Comp. Phys.* **221**, 349–369 (2007).
- [87] G.E. Hale, *Astrophys. J.* **28**, 315–345 (1908).
- [88] J.F. Hawley, *Phys. Plasmas* **10**, 1946–1953 (2003).
- [89] H. Harder and U. Hansen, *Geophys. J. Intern.* **161**, 522–532 (2005).
- [90] A. Herzenberg, *Philos. Trans. R. Soc. London* **A250**, 543–585 (1958).
- [91] R. Hollerbach, *Phys. Earth Planet. Int.* **98**, 163–185 (1996).
- [92] R. Hollerbach and G. Rüdiger, *Phys. Rev. Lett.* **95**, 124502 (2005).
- [93] R. Hollerbach, E. Canet, and A. Fournier, *Eur. J. Mech. B/Fluids* **26**, 729–737 (2007).
- [94] P. Hoyng and J.J. Duistermaat, *EPL* **68**, 177–183 (2004).
- [95] D. R. Inglis, *Rev. Mod. Phys.* **53**, 481–496 (1981).
- [96] A.B. Iskakov, S. Descombes, and E. Dormy, *J. Comp. Phys.* **197**, 540–554 (2004).
- [97] D.J. Ivers and R.W. James, *Geophys. Astrophys. Fluid Dyn.* **44**, 271–278 (1988).
- [98] H. Ji, M Yamada, S. Hsu, and R. Kulsrud, *Phys. Rev. Lett.* **80**, 3256–3259 (1998).
- [99] H. Ji et al., *Phys. Plasmas* **3**, 1935–1942 (1996).
- [100] H. Ji, J. Goodman, and A. Kageyama, *Mon. Not. Roy. Astr. Soc.* **325**, L1–L5 (2001).
- [101] H. Ji, M. Burin, E. Scharfman, and J. Goodman, *Nature* **444**, 343–346 (2006).
- [102] H. Ji, J. Goodman, and A. Kageyama, *Mon. Not. Roy. Astron. Soc.* **325**, L1–L5 (2001).
- [103] A. Kageyama, M. M. Ochi, and T. Sato, *Phys. Rev. Lett.* **82**, 5409–5412 (1999).
- [104] R. Kaiser, *Geophys. Astrophys. Fluid Dyn.* **101**, 185–197 (2007).
- [105] S. Kenjereš, K. Hanjalić, S. Renaudier, F. Stefani, G. Gerbeth, and A. Gailitis, *Phys. Plasmas* **13**, 122308 (2006).
- [106] S. Kenjereš and K. Hanjalić, *Phys. Rev. Lett.* **98**, 104501 (2007).
- [107] S. Kenjereš and K. Hanjalić, *New J. Phys.* **9**, 306 (2007).
- [108] I.V. Khalzov, *Tech. Phys.* **76**, 26 (2006).
- [109] I.V. Khalzov, V.I. Ilgisonis, A.I. Smolyakov, and E.P. Velikhov, *Phys. Fluids* **18**, 124107 (2006).
- [110] I.V. Khalzov, A.I. Smolyakov, and V.I. Ilgisonis, arXiv:0711.2818 (2007).
- [111] I.M. Kirko, G.E. Kirko, A.G. Sheinkman, and M.T. Telichko, *Dokl. Akad. Nauk. SSSR*, **266**, 854–856 (1982).
- [112] O.N. Kirillov, *Int. Journ. Non-Linear Mech.* **42**, 71–87 (2007).
- [113] L.I. Kitchatinov and G. Rüdiger, *Astron.* **329**, 372–375 (2008).
- [114] M.G. Kivelson et al., *Nature* **384**, 537–541 (1996).
- [115] E. Knobloch, *Mon. Not. R. Astron. Soc.* **255**, P25–P28 (1992).
- [116] M. Kono and P.H. Roberts, *Rev. Geophys.* **40**, 1013 (2002).
- [117] C. Kouveliotou et al., *Nature* **393**, 235–237 (1998).
- [118] D.S. Krasnov, E. Zienicke, O. Zikanov, T. Boeck, and A. Thess, *J. Fluid Mech.* **504**, 183–211 (2004).
- [119] F. Krause and K.-H. Rädler, *Mean-field magnetohydrodynamics and dynamo theory* (Akademie, Berlin, 1980).
- [120] P.P. Kronberg, Q.W. Dufton, H. Li, and S.A. Colgate, *Astrophys. J.* **560**, 178–186 (2001).
- [121] R. Krechetnikov and J.E. Marsden, *Rev. Mod. Phys.* **79** 519–553 (2007).
- [122] W. Kuang and J. Bloxham, *Nature* **389**, 371–374 (1997).
- [123] R.M. Kulsrud and E.G. Zweibel, *Rep. Progr. Phys.* **71**, 046901 (2008).

- [124] R. Laguerre, C. Nore, J. Léorat, J.L. Guermond, C.R. Mec. **334**, 593-598 (2006).
- [125] R. Laguerre et al., Phys. Rev. Lett. **101**, 104501 (2008).
- [126] V.P. Lakhin and E.P. Velikhov, Phys. Lett. A **369** 98-106 (2007).
- [127] J. Larmor, Rep. Brit. Assoc. Adv. Sci., 159–160 (1919).
- [128] D.P. Lathrop, W.L. Shew, and D.R. Sisan, Plasma Phys. Contr. Fusion **43**, A151-A160 (2001).
- [129] J.-P. Laval, P. Blaineau, N. Leprovost, B. Dubrulle, F. Daviaud, Phys. Rev. Lett. **96**, 204503 (2006).
- [130] B. Lehnert, Arkiv för Fysik **13**, 10, 109–116 (1958).
- [131] B. Lehnert, in: *Magnetohydrodynamics: Historical Evolution and Trends*, edited by S. Molokov, R. Moreau, H.K. Moffatt (Springer, Dordrecht, 2007), pp. 27-36.
- [132] J. Léorat, F. Rigaud, R. Vitry and G. Herpe, Magnetohydrodynamics **39**, 321-326 (2003).
- [133] J. Léorat, Magnetohydrodynamics **42**, 143-151 (2006).
- [134] J.T.C. Liu, Ann. Rev. Fluid Mech. **21**, 285-315 (1988).
- [135] W. Liu, J. Goodman, I. Herron, and H.T. Ji, Phys. Rev. E **74**, 056302 (2006).
- [136] W. Liu, J. Goodman, and H. Ji, Phys. Rev. E **76**, 016310 (2007).
- [137] W. Liu, Astrophys. J. **684**, 515-524 (2008).
- [138] F.J. Lowes and I. Wilkinson, Nature **198**, 1158–1160 (1963).
- [139] F.J. Lowes and I. Wilkinson, Nature **219**, 717–718 (1968).
- [140] Lucretius Carus, Titus, On the nature of things, Project Gutenberg Etext (www.gutenberg.org/etext/785), translated by William Ellery Leonard
- [141] L. Marié et al., in *Dynamo and Dynamics, a Mathematical Challenge*, edited by P. Chossat, D. Armbruster, and I. Oprea (Kluwer, Dordrecht/Boston/London, 2001), pp. 35–50.
- [142] L. Marié, J. Burguete, F. Daviaud, and J. Léorat, Eur. Phys. J. B **33m** 469-485 (2003).
- [143] L. Marié, C. Normand, and F. Daviaud, Phys. Fluids **18**, 017102 (2006).
- [144] R.T. Merrill, R. T., M. W. McElhinny, and Ph. L. McFadden, *The magnetic field of the earth : paleomagnetism, the core, and the deep mantle* (Academic, San Diego, 1998).
- [145] H.K. Moffatt, *Magnetic field generation in electrically conducting fluids* (Cambridge University, Cambridge, 1978).
- [146] R. Monchaux et al., Phys. Rev. Lett. **98**, 044502 (2007).
- [147] P. Moresco and T. Alboussiere, J. Fluid Mech. **504**, 167-181 (2004).
- [148] M. Morris, K. Uchida, and T. Do, Nature **440**, 308-310 (2006).
- [149] U. Müller and R. Stieglitz, Naturwissenschaften **87**, 381–390 (2000).
- [150] U. Müller and R. Stieglitz, Nonl. Proc. Geophys. **9**, 165-170 (2002).
- [151] U. Müller, R. Stieglitz, and S. Horanyi, J. Fluid Mech. **498**, 31-71 (2004).
- [152] U. Müller, R. Stieglitz, and S. Horanyi, J. Fluid Mech. **552**, 419-440 (2006).
- [153] H.-C. Nataf et al., Geophys. Astrophys. Fluid Dyn. **100**, 281-298 (2006).
- [154] T. Nakajima and M. Kono, Geophys. Astrophys. Fluid Dynamics **60**, 177–209 (1991).
- [155] J. Needham, *Science and Civilisation in China*, (Cambridge University, Cambridge, 1962), vol. 4, part 1.
- [156] N.F. Ness, K. W. Behannon, R. P. Lepping, and Y. C. Whang, Nature **255**, 204–205 (1975).
- [157] M.D. Nornberg, E.J. Spence, R.D. Kendrick, C.M. Jacobson, and C.B. Forest, Phys. Rev. Lett. **97**, 044503 (2006).
- [158] M.D. Nornberg, E.J. Spence, R.D. Kendrick, C.M. Jacobson, and C.B. Forest, Phys. Plasmas **13**, 055901 (2006).
- [159] G.I. Ogilvie and A.T. Potter, Phys. Rev. Lett. **100**, 074503 (2008).
- [160] M. Ossendrijver, Astron. Astrophys. Rev. **11**, 287-367 (2003).
- [161] E.N. Parker, Astrophys. J. **122**, 293-314 (1955).
- [162] N.L. Peffley, A.B. Cawthorne, and D.P. Lathrop, Phys. Rev. E. **61**, 5287–5294 (2000).
- [163] N.L. Peffley, A. G. Goumievski, A. B. Cawthorne, and D. P. Lathrop, Geophys. J. Int. **141**, 52–58 (2000).
- [164] C.L. Pekeris, Y. Accad, and B Shkoller, Phil. Trans. R. Soc. Lond. **A275**, 425–461 (1973).
- [165] M.E. Pessah and D. Psaltis, Astrophys. J. **628**, 879-901 (2005).
- [166] F. Pétrélis, M. Bourgoïn, L. Marié, J. Burguete, A. Chiffaudel, F. Daviaud, S. Fauve, P. Odier, and J.-F. Pinton, Magnetohydrodynamics **38**, 163-176 (2002).
- [167] F. Pétrélis et al., Phys. Rev. Lett. **90**, 174501 (2003).
- [168] F. Pétrélis, N. Mordant, and S. Fauve, Geophys. Astrophys. Fluid Dyn. **101**, 289-323 (2007).
- [169] Petrus Peregrinus de Maricourt, *Opera* (Scuola normale superiore, Pisa, 1995).
- [170] F. Plunian, P. Marty P, and A. Alemany, J. Fluid Mech. **382**, 137–154 (1999).
- [171] E.S. Pierson, E. S., Nucl. Sci. Eng. **57**, 155–163 (1975).
- [172] Yu.B. Ponomarenko, J. Appl. Mech. Tech. Phys. **14**, 775–779 (1973).
- [173] J. Priede, I. Grants, and G. Gerbeth, Phys. Rev. E **75**, 047303 (2007).
- [174] J. Priede and G. Gerbeth, in preparation
- [175] K.-H. Rädler, E. Apstein, M. Rheinhardt, and M. Schüler, Studia geoph. et geod. **42**, 1–9 (1998).
- [176] K.-H. Rädler, M. Rheinhardt, E. Apstein, and H. Fuchs, Magnetohydrodynamics **38**, 41-71 (2002).
- [177] K.-H. Rädler, M. Rheinhardt, E. Apstein, and H. Fuchs, Magnetohydrodynamics **38**, 73-94 (2002).
- [178] K.-H. Rädler, M. Rheinhardt, E. Apstein, and H. Fuchs, Nonl. Proc. Geophys. **9**, 171-187 (2002).
- [179] K.-H. Rädler and M. Rheinhardt, Magnetohydrodynamics **38**, 211-217 (2002).
- [180] K.-H. Rädler and M. Rheinhardt, Geophys. Astrophys. Fluid Dyn. **101**, 117-154 (2007).
- [181] F. Ravelet, A. Chiffaudel, F. Daviaud, J. Léorat, Phys. Fluids **17**, 117104 (2005).
- [182] F. Ravelet, *Von Karman flow and the dynamo effect*, Thesis (Ecole Polytechnique, 2005), <http://tel.archives-ouvertes.fr/tel-00011016/en/>.

- [183] F. Ravelet et al., arXiv:0704.2565
- [184] Rayleigh Lord, *On the dynamics of revolving fluids* Scientific papers **6**, 447-453 (1929).
- [185] A.B. Reighard and M. R. Brown, Phys. Rev. Lett. **86**, 2794–2797 (2001).
- [186] F. Rincon, G.I. Ogilvie, and M.R.E. Proctor, Phys. Rev. Lett. **98**, 254502 (2007).
- [187] A. Roach, H. Ji, W. Liu, and J. Goodman, Bull. Amer. Phys. Soc. **52**, No. 11, BP8.00084 (2007).
- [188] G.O. Roberts, Philos. Trans. R. Soc. London, **A271**, 411–454 (1972).
- [189] P.H. Roberts, P. H., in *Lectures on Solar and Planetary Dynamos*, edited by M. R. E. Proctor and A. D. Gilbert, (Cambridge University, Cambridge, 1994), pp. 1–58.
- [190] P.H. Roberts and T. H. Jensen, Phys. Fluids B **7**, 2657–2662 (1992).
- [191] P.H. Roberts and A. M. Soward, Annu. Rev. Fluid Mech. **24**, 459–512 (1992).
- [192] P.H. Roberts and G. A. Glatzmaier, Rev. Mod. Phys. **72**, 1081–1123 (2002).
- [193] G. Rüdiger and R. Hollerbach, *The Magnetic Universe* (Wiley, Berlin, 2004).
- [194] G. Rüdiger, R. Hollerbach, M. Schultz, and D.A. Shalybkov, Astron. Nachr. **326**, 409-413 (2005).
- [195] G. Rüdiger and R. Hollerbach, Phys. Rev. E **76**, 068301 (2007).
- [196] G. Rüdiger, R. Hollerbach, M. Schultz, and D. Elstner, Mon. Not. R. Astron. Soc. **377**, 1481-1487 (2007).
- [197] G. Rüdiger et al., Astrophys. J. **649**, L145-L147 (2006).
- [198] A.A. Schekochihin and S.C. Cowley, Phys. Plasmas **13**, 056501 (2006).
- [199] A.A. Schekochihin et al., New J. Phys. **9**, 3000 (2007).
- [200] F. Schultz-Grunow, ZAMM **39**, 101-110 (1959).
- [201] D. Schmitt et al., J. Fluid Mech. **604**, 175-197 (2008).
- [202] M. Schrunner, K.-H. Rädler, D. Schmitt, M. Rheinhardt, and U. Christensen, Astron. Nachr. **326**, 245-249 (2005).
- [203] M. Schrunner, K.-H. Rädler, D. Schmitt, M. Rheinhardt, and U. Christensen, Geophys. Astrophys. Fluid Dyn. **101**, 81-116 (2007).
- [204] N.I. Shakura and R.A. Sunyaev, Astron. Astrophys. **24**, 337-355 (1973).
- [205] W.L. Shew, W. L., D. R. Sisan, and D. P. Lathrop, in *Dynamo and Dynamics, a Mathematical Challenge*, edited by P. Chossat, D. Armbruster, and I. Oprea (Kluwer, Dordrecht/Boston/London, 2001), pp. 83–92.
- [206] W.L. Shew and D.P. Lathrop, Phys. Earth Planet. Inter. **153**, 136-149 (2005).
- [207] A. Shukurov and D.D. Sokoloff, in *The Cosmic Dynamo*, edited by F. Krause et al. (IAU, 1993), pp. 367-371.
- [208] C.W. Siemens, Proc. R. Soc. London **15**, 367 (1867).
- [209] Simonyi, K., *Kulturgeschichte der Physik*, (Urania, Leipzig/Jena/Berlin, 1990), p. 343.
- [210] D.R. Sisan, W.L. Shew, and D.P. Lathrop, Phys. Earth Planet. Inter. **135**, 137-159 (2003).
- [211] D.R. Sisan et al., Phys. Rev. Lett. **93**, 114502 (2004).
- [212] D.J. Southwood, Planet. Space Sci. **45**, 113–117 (1997).
- [213] E.J. Spence, M.D. Nornberg, C.M. Jacobson, R.D. Kendrick, and C.B. Forest, Phys. Rev. Lett. **96**, 055002 (2006).
- [214] E.J. Spence et al., Phys. Rev. Lett. **98**, 164503 (2007).
- [215] H.C. Spruit, Astron. Astrophys. **381**, 923-932 (2002).
- [216] M. Steenbeck, F. Krause, and K.-H. Rädler, Z. Naturforsch. **21a**, 369–376 (1966).
- [217] M. Steenbeck, I. M. Kirko, A. Gailitis, A. P. Klawina, F. Krause, I. J. Laumanis, and O. A. Lielausis, Mber. Dt. Ak. Wiss. **9**, 714–719 (1967).
- [218] M. Steenbeck, Letter to H. Klare, President of the Academy of Sciences of the GDR (1975).
- [219] F. Stefani, G. Gerbeth, and A. Gailitis, in *Transfer Phenomena in Magnetohydrodynamic and Electroconducting Flows*, edited by A. Alemany, Ph. Marty, J. P. Thibault (Kluwer, Dordrecht/Boston/London, 1999) pp. 31–44.
- [220] F. Stefani, G. Gerbeth, and K.-H. Rädler, Astron Nachr. **321**, 65-73 (2000).
- [221] F. Stefani and G. Gerbeth, Phys. Rev. Lett. **94**, 184506 (2005).
- [222] F. Stefani, G. Gerbeth, U. Günther, and M. Xu, Earth Planet. Sci. Lett. **243**, 828-840 (2006).
- [223] F. Stefani et al., Eur. J. Mech. B/Fluids **25**, 894-908 (2006).
- [224] F. Stefani, M. Xu, L. Sorriso-Valvo, G. Gerbeth, and U. Günther, Geophys. Astrophys. Fluid Dyn. **101**, 227-248 (2007).
- [225] F. Stefani et al., Phys. Rev. Lett. **97**, 184502 (2006).
- [226] F. Stefani et al., New J. Phys. **9**, 295 (2007).
- [227] F. Stefani et al., Astron. Nachr. **329**, 652 (2008).
- [228] R. Stepanov et al., Phys. Rev. E **73**, 046310 (2006).
- [229] F. Stefani and G. Gerbeth, in *MHD Couette Flows. Experiments and Methods*, edited by A. Bonanno, R. Rosner and G. Rüdiger (AIP Conference Proceedings 733, 2004), pp. 100-113.
- [230] S. Stellmach and U. Hansen, Phys. Rev. E **70**, 056312 (2004).
- [231] S. Stellmach and U. Hansen, Geochem. Geophys. Geosyst. **9**, Q05003 (2008).
- [232] D.J. Stevenson, Rep. Progr. Phys. **46**, 555-620 (1983).
- [233] D.J. Stevenson, Earth Planet. Sci. Lett. **208**, 1-11 (2003).
- [234] R. Stieglitz and U. Müller, Phys. Fluids **13**, 561–564 (2001).
- [235] J. Szklarski and G. Rüdiger, Astron Nachr. **327**, 844-849 (2006).
- [236] J. Szklarski, Astron Nachr. **328**, 499-506 (2007).
- [237] R. J. Tayler, Mon. Not. R. Astron. Soc. **161**, 365-380 (1973).
- [238] A. Tilgner, Acta Astron. et Geophys. Univ. Comenianae **XIX**, 51–62 (1997).
- [239] A. Tilgner, Phys. Lett. A **226**, 75–79 (1997).
- [240] A. Tilgner, Phys. Earth Planet. Inter. **117**, 171–177 (2000).
- [241] A. Tilgner and F. H. Busse, in *Dynamo and Dynamics, a Mathematical Challenge*, edited by P. Chossat, D. Armbruster, and I. Oprea (Kluwer, Dordrecht/Boston/London, 2001), pp. 109–116.

- [242] A. Tilgner, Phys. Rev E **66**, 017304 (2002).
- [243] A. Tilgner, Phys. Fluids **14**, 4092-4094 (2002).
- [244] A. Tilgner, Phys. Fluids **17**, 034104 (2005).
- [245] N.J. Turner, T. Sano, and N. Dziourkevitch, Astrophys. J. **659**, 729-737 (2007).
- [246] Y.V. Vandakurov, Soviet Astron. **16**, 265 (1972).
- [247] E.P. Velikhov, Sov. Phys. JETP **36** 995-998 (1959).
- [248] E.P. Velikhov, Phys. Lett. A. **358**, 216-221 (2006).
- [249] M.K. Verma, Phys. Rep. **401**, 229-380 (2004).
- [250] R. Volk, P. Odier, and J.-F. Pinton, Phys. Fluids **18**, 085105 (2006).
- [251] Z. Wang, V.I. Pariev, C.W. Barnes, and D.C. Barnes, Phys. Plasmas **9**, 1491-1494 (2002).
- [252] T. Weier, V. Shatrov, and G. Gerbeth, in: *Magnetohydrodynamics: Historical Evolution and Trends*, edited by S. Molokov, R. Moreau, H.K. Moffatt (Springer, Dordrecht, 2007), pp. 295-312.
- [253] G. Wendt, Ing.-Arch. **4**, 577-595 (1933).
- [254] J. Wicht and P. Olson, Geochem. Geophys. Geosyst. **5**, Q03H10 (2004).
- [255] I. Wilkinson, Geophys. Surveys **7**, 107-122 (1984).
- [256] F. Winterberg, Phys. Rev. **131**, 29-37 (1963).
- [257] C. Wheatstone, Proc. R. Soc. London **15**, 369 (1867).
- [258] J. Wosnitza et al., J. Mag. Magn. Mat. **310**, 2728-2730 (2007).
- [259] M. Xu, F. Stefani, and G. Gerbeth, J. Comp. Phys. **196** 102-125 (2004).
- [260] M. Xu, F. Stefani, and G. Gerbeth, Phys. Rev. E **70**, 056305 (2004).
- [261] M. Xu, F. Stefani, and G. Gerbeth, J. Comp. Phys. **227**, 8130-8144 (2008).
- [262] P.J. Zandbergen and D. Dijkstra, Ann. Rev. Fluid Mech. **19**, 465-491 (1987).